TÉCNICO LISBOA

Bosonic Stars:

Scalar and Vector Field Self-Gravitating Configurations

Miguel Castilho Soares Duarte

Thesis to obtain the Master of Science Degree in

Engineering Physics

Supervisors: Professor Doutor Vítor Manuel dos Santos Cardoso
Doutor Richard Pires Brito

Examination Committee

Chairperson: Professor Doutor José Pizarro de Sande e Lemos
Supervisor: Professor Doutor Vítor Manuel dos Santos Cardoso
Member of the Committee: Doutor Vincenzo Vitagliano

July 2016

Ao Filipe e à Mariana pelo interesse incessante,
Aos meus amigos pela inabalável confiança,
À avó Isabel pelas humildes conversas,
Ao Chico e à Gi por tudo o que sou.

Acknowledgments

The very first person I must thank is Richard Brito. His endless patience, together with his deep and vast knowledge of physics, taught me a great deal of what I know today. Second of all, I want to thank Prof. Vítor Cardoso for the oportunity and incentive to be a part of the exciting work done by GRIT.

Although a simple 'thank you' seems rather inadequate, I would thank my parents, my brother and my sister. They are the ones to blame for the boldness to pursue a physicist's life. Furthermore, the support shown by the many friends with whom I had the priviledge to cross paths has been entirely defining in the confidence I have to face challenges.

Last but not least, I would like to thank my grandmother for always being there, ready to share wisdom and humility.

Resumo

Configurações de partículas sem spin confinadas pela gravidade, ou estrelas de bosões escalares, têm sido estudadas desde há décadas e têm hoje várias aplicações que incluem desde considerá-las possíveis candidatos a matéria escura a indicações de que estas terão representado um papel importante no desenvolvimento do Universo primordial. Estes objectos também foram investigados em espaços-tempo assimptoticamente Anti-de Sitter (AdS), devido nomeadamente à correspondência AdS/CFT, uma aparente coerência entre fenómenos físicos em AdS e teorias de campo conformes.

Neste trabalho são estudadas soluções de estrelas de bosões escalares bem como configurações de partículas de spin-1, as chamadas estrelas Proca. Estas são construídas em espaços-tempo assimptoticamente planos e em AdS de modo a evidenciar as diferenças entre os dois. Tais soluções são encontradas numericamente e comparadas com resultados analíticos encontrados no limite em que os campos massivos podem ser considerados como perturbações da métrica em vácuo. Configurações de spin-1 são estudadas em cinco dimensões e é argumentado que estas são sempre instáveis em espaço plano.

Condições de estabilidade face a perturbações lineares esfericamente simétricas são encontradas para estrelas Proca em ambos os espaços-tempo. Por fim, um teorema do cabelo é provado para estrelas Proca em AdS estabelecendo que o único buraco negro possível em simetria esférica é o espaço-tempo de Schwazschild-AdS.

Alguns dos resultados obtidos na realização desta tese encontram-se em [1].

Palavras-chave: assimptoticamente AdS, campos bosónicos, estrela de bosões, estrela Proca, buraco negro.

Abstract

The study of scalar boson stars, self-gravitating configurations of spinless particles, has been ongoing for decades and these have found numerous applications that range from considering them as plausible dark matter candidates, to indications that these might have played an important part in the development of the early Universe. These objects have also been investigated extensively in asymptotically Anti-de Sitter (AdS) spacetimes, mainly due to the AdS/CFT correspondence, an apparent coherence between physical phenomena in AdS and conformal field theories.

In this work we study solutions of scalar boson stars as well as configurations made of spin-1 particles, the so called Proca stars. These are constructed in asymptotically flat spacetimes and in AdS in order to assert the differences between the two. Such solutions are found numerically and then compared with analytical results recovered by considering the matter fields as perturbations of the vacuum metric. Spin-1 configurations are constructed in five dimensions and an instability of these solutions in flat spacetimes is argued.

Furthermore, stability conditions are asserted for Proca stars in both spacetimes against linear spherically symmetric perturbations of the metric and the fields. Finally, a no-hair theorem is proved for Proca stars in AdS, stating that the only possible black hole in spherical symmetry is the Schwarzschild-AdS spacetime.

Some of the results obtained throughout this thesis can be found in [1].

Keywords: asymptotically AdS, bosonic fields, boson star, Proca star, black hole.

Contents

List of Figures

Chapter 1

Introduction

1.1 Overview and Motivation

In 1955, John Wheeler proposed the existence of configurations of photons or gravitons confined by Einstein's gravity, which he called *geons* [2]. These were soon found to be unstable. Just over a decade later, Kaup was inspired by this idea and was able to find stable solutions replacing the electromagnetic field with a complex scalar field [3]. These gravitationally bound spherically symmetric equilibrium configurations of complex scalar fields are nowadays known as boson stars.

Over the following years, there was substantial activity in cosmology and particle physics on the possibility of a critical role played by fundamental scalar fields in the development of the early Universe. Most attempts to model inflation make use of scalar fields as the *inflaton* field, the vacuum energy ultimately responsible for the exponential inflation of the Universe (see for example Ref. [4] or Ref. [5] for a review of cosmic inflation).

Studies of stellar rotation in various galaxies describe the dependence between the rotation speed at a given radius and the mass contained within that radius. The observation that the rotation curve becomes flat for large radius suggests the existence of a large dark matter halo as the only possible mechanism to hold the galaxy together. Boson stars have been largely called upon to solve this problem as they can be matched to observational constraints for galactic dark matter halos [6, 7].

Yet another application of these objects consists in conceiving them as black hole mimickers [8]. Several indications have pointed towards the possibility that some of the detected astrophysical objects assumed to be black holes might indeed be massive boson stars. This is a question gravitational wave observation might be able to settle [9, 10]. As boson stars allow for orbits inside what would be an event horizon in the case of a black hole, geodesics would show extreme pericenter precession that would result in considerably different gravitational wave emission [11].

In recent years there have also been proposals advocating for massive spin-1 particles as dark matter candidates [12, 13, 14]. Self-gravitating configurations of such particles are called Proca stars [15], as they employ the relativistic field equations named after Alexandru Proca that describe the behaviour or these particles [16]. These stars can be thought of as a massive version of Wheeler's *geon* idea.

As scalar boson stars have seen more than five decades of extensive study, Proca stars represent an entirely new field of study in many ways analogous to that of their spinless counterpart.

In this work, besides asymptotically flat spacetimes, self-gravitating configurations are studied in a background spacetime characterized by a negative cosmological constant, Anti-de Sitter (AdS) spacetime. In recent years we have witnessed the interest in physical phenomena in AdS spacetimes rise tremendously, mainly due to the apparent correspondence between the propagation of gravitating matter fields in AdS and the physical effects of a conformal field theory (CFT) in the boundary of that spacetime. This correspondence, usually referred to as the AdS/CFT correspondence, was proposed by Maldacena in 1998 [17].

An additional motivation to investigate the physics of such a spacetime is the fact that AdS is maximally symmetric, which makes it an excelent model for investigating questions of principle such as the quantization of fields in a curved spacetime. Given the confining nature of the AdS boundary, asymptotically AdS (aAdS) spacetimes are an excellent testbed to study strong-gravity effects in confined geometries. Moreover, several dynamical studies in this spacetime point towards a nonlinear instability against black hole formation for general sets of smooth initial data regardless of their initial amplitude [18, 19, 20]. Although, it is now clear that there exist large classes of initial configurations that do not collapse gravitationally, some of which are boson stars [21, 22, 23, 24, 25].

It is useful to study higher-dimensional gravitational effects and, in particular, five-dimensional ones, not only to improve our understanding on how the behaviour of physical systems depends on dimensionality, but also in the context of the AdS/CFT correspondence, as the conformal field theory is valid only for the boundary of the AdS spacetime. Hence, considering self-gravitating matter fields in a five-dimensional spacetime results in a four-dimensional conformal field theory.

To the extent of my knowledge, despite the extensive work that has already been done on scalar fields in aAdS spacetimes, there is still no information available in the literature concerning the properties of complex vector fields in that spacetime.

1.2 Thesis Outline

This thesis is organized as follows. Chapter 2 is an overview of all the work that has already been done concerning bosonic stars in AdS and in flat spacetimes. Chapter 3 shows the numerical construction of scalar boson star and Proca star solutions in asymptotically flat spacetimes. On chapter 4, the same procedure is applied for aAdS spacetimes with different values of Λ. The main differences in the behaviour os such structures with the two different asymptotics are established. Also, a no-hair theorem for Proca stars in AdS is proved in detail on Appendix B. Section 4.3 shows the construction of numerical solutions of Proca stars in a five-dimensional AdS spacetime and compares them with solutions found for asymptotically flat spacetime. An instability of all five-dimensional Proca stars for $\Lambda = 0$ is argued.

Analytical solutions are found on chapter 5 in the small field amplitude regime in AdS so as to enable comparison with the solutions obtained numerically, thus validating the numerical method. Extrapolating this validity to outside the considered approximation grants confidence in the results.

Finally, chapter 6 shows a full study of the stability of Proca stars in both considered spacetimes against small linear spherically symmetric perturbations. Stability conditions are established for these solutions.

Chapter 2

State of the art

2.1 Scalar boson stars in asymptotically flat spacetime

A widely known theorem proved by Derrick in 1964 [26] uses a clever scaling argument to show that no regular static non-topological localized scalar field solutions are stable in flat space (a detailed proof is shown in Appendix A). One way of avoiding this constraint is dropping staticity and coupling the scalar field to gravity. One can then consider a scalar field given by

$$\phi(t,r) = \phi_0(r)e^{-i\omega t}\,. \tag{2.1}$$

It can be shown that, although the field is not static anymore, the spacetime is, so that the star itself is a stationary soliton-like solution. This is only possible for a complex field which makes the stress-energy tensor static[1]. If the field is otherwise taken to be real, the stress-energy tensor is not static anymore and only oscillatory solutions are feasible.

Boson stars were first constructed in the ground-breaking work done by Kaup [3] and soon after by Ruffini and Bonazzola [27]. These objects, in their simplest version, are macroscopic spherically symmetric quantum states of non-interacting particles with only the Heisenberg uncertainty principle preventing them from collapsing into a black hole. Subsequently, interesting work was done introducing self-interaction potentials in the Lagrangian of the system, in particular, in Ref. [28], a potential proportional to the fourth power of the scalar field was added as an interaction term (see also [29]). In the case of a repulsive interaction, for example, the solutions kept the same qualitative behaviour as in the non-interacting case, simply increasing the critical mass and particle number. Further departures from the original idea include the work done by Jetzer and Van der Bij extending the model to include a U(1) gauge charge [30] and a study of boson-fermion stars [31], self-gravitating configurations of a mixture of bosonic and fermionic matter.

Stability against charge-conserving small radial perturbations has been discussed by Gleiser in Ref. [32] and by Lee and Pang in [33]. A study of asymptotically flat, rotating boson stars is presented

[1] Note that, if all the terms in the stress-energy tensor are proportional to the field or its derivatives and their complex conjugate, the time dependence cancels out.

in [34] and a recent detailed review on the dynamics of boson stars is given in [35].

It is worth mentioning an argument devised by Landau [36] in order to obtain an estimate for the maximum mass of a star. This argument was first used for a fermion star, but the same outline can be used for a boson star. For comparison, both are shown below.

Suppose there is a configuration of N fermions within a radius R so that the number density is $n \sim N/R^3$. If we consider the volume per fermion to be $\sim 1/n$, the Heisenberg uncertainty principle yields a momentum of $\sim \hbar n^{1/3}$, which in turn gives a Fermi energy of

$$E_F \sim \frac{\hbar c N^{1/3}}{R} \,. \tag{2.2}$$

The gravitational energy is given by

$$E_G \sim \frac{GMm_B}{R} \,, \tag{2.3}$$

where $M = Nm_B$ and m_B is the baryon mass. So, the total energy is

$$E \sim \frac{\hbar c N^{1/3}}{R} - \frac{GNm_B^2}{R} \,. \tag{2.4}$$

Note that, when E is positive (small N), E_F is decreased by increasing R and the particles eventually become non-relativistic ($E_F \sim 1/R^2$). Therefore, for a finite R, E becomes negative but goes to zero as R increases, so there must be a stable equilibrium at some R. On the other hand, when E is negative (large N), it can be decreased without bound. Hence, the equilibrium with maximum N is reached at $E = 0$.

The maximum number of baryons and the maximum mass are then

$$N_{max} \sim \left(\frac{\hbar c}{Gm_B^2}\right)^{3/2} = M_{Pl}^3/m_B^3 \,, \tag{2.5}$$

$$M_{max} \sim N_{max} m_B = M_{Pl}^3/m_B^2 \,, \tag{2.6}$$

respectively, where M_{Pl} is the Planck mass. As an example, if we take neutrons to be the baryons this star is composed of, we get $M_{max} \sim 1.85\ M_\odot$.

To find an estimate for the maximum mass of a boson star, one can take $\Delta p \Delta x \geq \hbar$ and consider $\Delta x = R$. Taking the maximum momentum to be $\Delta p = m_B c$, we get

$$m_B c R \geq \hbar \,. \tag{2.7}$$

The maximum possible mass will saturate the uncertainty bound and drive the radius of the star towards its Schwarzschild radius $R_S = 2GM/c^2$. Substituting yields

$$M_{max} \sim \frac{1}{2}\frac{\hbar c}{Gm_B} = 0.5\ M_{Pl}^2/m_B \,. \tag{2.8}$$

Numerical studies in Ref. [27] show a maximum mass of about $0.633\ M_{Pl}^2/m_B$, which is fairly close to

the estimate in (2.8). To enable comparison between bosons and fermions, we consider hypothetical bosons with the mass of a neutron and we get $M_{max} \sim 7.1 \times 10^{-20}\ M_{\odot}$. Hence, the maximum mass is, in general, much larger for the case of a fermion star than for that of a boson star.

2.1.1 Oscillatons

As shown by Derrick's theorem, static real scalar field solutions cannot exist in an asymptotically flat spacetime. However, there are non-singular time-dependent near-equilibrium configurations of self-gravitating real scalar fields called Oscillatons. These objects are quite similar to boson stars both in nature and behaviour, with the important exception that the fields they contain are real and there is a time-dependence in order to avoid singularities. This time-dependence is present in both the metric and the scalar field, as they both oscillate. Oscillatons were first considered in the numerical work done by Seidel and Suen [37].

An interesting peculiarity of these solutions is that they are not truly stable configurations, in fact they emit radiation and decay. However, the decay timescales are so large (typically much larger than the age of the Universe) that, for all purposes, they can be considered stable [38, 39].

2.2 Proca stars in asymptotically flat spacetime

In reference [15] it was found that Proca star solutions show the same qualitative behaviour as their spinless counterpart with a larger critical mass and particle number, namely, the maximum mass is of $1.058\ M_{Pl}^2/m_B$ for a non-interacting spherically symmetric Proca star. Stability against linear radial perturbations is studied with the result that these configurations are stable for a certain range of vibrational frequencies, bounded by the point of maximum mass. Finally, solutions with rotation are constructed.

More recently, rotating Proca stars were shown to be continuously connected to asymptotically flat rotating black holes with Proca hair [40].

2.3 Scalar boson stars in AdS

There is significantly less work available in the literature concerning the behaviour of boson stars in aAdS spacetimes than in asymptotically flat spacetimes. Nonetheless, in 1998, Sakamoto and Shiraishi obtained scalar field solutions in a (2+1)-dimensional spacetime with a negative cosmological constant [41].

Relevant work has also been done in this field by Astefanesei and Radu [42], where they provide a complete study of the basic properties of boson stars in an aAdS spacetime for an arbitrary number of spatial dimensions, much in the same way as was done for asymptotically flat spacetimes over the years. Ref. [42] establishes that these solutions are linearly stable for a certain interval of frequencies (analogous to the one found for Proca stars) and that the properties of boson stars subjected to a negative Λ do not change significantly, except for the fact that fields experience a complicated power

decay, instead of the normal exponential at spacial infinity. Also, in AdS, the critical mass decreases as the modulus of Λ increases. Finally, a general proof of a no-hair theorem is shown, stating that a D-dimensional static spherically symmetric aAdS black hole spacetime with an energy-momentum tensor satisfying the weak energy condition and $T^{\theta}_{\theta} \leq T^{r}_{r}$, is necessarily trivial (i.e. $T^{\nu}_{\mu} = 0$), meaning that the only possible black hole is the Schwarzschild-AdS spacetime.

Further work is presented in [18] concerning the time evolution of a free massless scalar field coupled to gravity in a four-dimensional aAdS spacetime, with the result that, from a large class of smooth initial data, black holes are formed, indicating that AdS is unstable (see also [19, 20]). This instability towards black hole formation takes place because more and more energy gets concentrated in the same region through weak turbulence. The existence of an instability of this sort is related to the particular causal structure of this spacetime, which is not globally hyperbolic, i.e., it does not have a Cauchy hypersurface. The main consequence of this peculiarity is that the perscription of initial data on a spacelike hypersurface in the usual way is not sufficient to fully determine its time evolution, so it is necessary to impose suitable boundary conditions on the timelike boundary of the AdS spacetime. In more intuitive terms, light takes a finite proper time to reach the AdS boundary, which is not the case in asymptotically flat spacetimes. This means that this boundary is in causal contact with the interior of the spacetime, thus affecting the behaviour of the physical systems.

Note, however, that boson stars seem to be immune to this instability for sufficiently small perturbations [21, 22, 23, 24, 25], which makes the study of these structures all the more interesting not only in the context of the AdS/CFT correspondence, but also to further extend our knowledge on the nature of the AdS instability.

Chapter 3

Numerical solutions in asymptotically flat spacetime

Scalar boson stars, as well as Proca stars, are constructed in an asymptotically flat spacetime. These solutions of the Einstein-Klein-Gordon and Einstein-Proca equations, respectively, are obtained numerically in order to obtain values for observables such as the ADM mass and the total number of particles of the star.

3.1 Scalar boson stars

Self-gravitating structures of non-interacting scalar particles can be seen as macroscopic quantum states with only the Heisenberg uncertainty principle preventing them from collapsing gravitationally. These are the simplest form of boson stars, just as Kaup first idealized them.

In the following calculations, we use approximately the same notation and ansatz as Ref. [32], in order to facilitate comparison of the resulting field equations.

3.1.1 Framework

Writing the action as

$$S = -\int d^4\sqrt{-g}\left(\frac{R}{16\pi G} - g^{\mu\nu}\Phi^*_{;\mu}\Phi_{;\nu} - \mu^2|\Phi|^2\right), \tag{3.1}$$

and varying it with respect to the metric $g^{\mu\nu}$ and the field Φ (with Φ^* its complex conjugate), we obtain Einstein's equations

$$R_{\mu\nu} - \frac{1}{2}g_{\mu\nu}R = 8\pi G T_{\mu\nu}\,, \tag{3.2}$$

with the energy-momentum tensor given by

$$T_{\mu\nu} = \Phi^*_{,\mu}\Phi_{,\nu} + \Phi^*_{,\nu}\Phi_{,\mu} - g_{\mu\nu}(g^{\alpha\beta}\Phi^*_{,\alpha}\Phi_{,\beta} - \mu^2|\Phi|^2)\,, \tag{3.3}$$

and the Klein-Gordon equation

$$g^{\mu\nu}\Phi_{;\mu\nu} + \mu^2\Phi = 0\,. \tag{3.4}$$

The Lagrangian density in question is invariant under a global phase rotation $\Phi \to \Phi e^{-i\alpha}$, which implies the existence of a conserved current

$$j^\mu = ig^{\mu\nu}(\Phi^*_{,\nu}\Phi - \Phi_{,\nu}\Phi^*)\,, \tag{3.5}$$

and a conserved Noether charge, namely the number of particles

$$Q = \int_\Sigma d^3x\sqrt{-g}j^t\,, \tag{3.6}$$

where j^t is the time component of the 4-current and Σ is a spacelike hypersurface.

3.1.2 Equations of motion and boundary conditions

The concept of star implies a configuration of matter that remains localized over time. Hence, one has to look for a localized structure such that the gravitational field is stationary and everywhere regular. For equilibrium configurations, the metric functions are time-independent and $\Phi(t,r) = \phi(r)e^{-i\omega t}$, where ω is a real frequency parameter. Recall that describing the scalar field in this way prevents contraints imposed by Derrick's theorem.

Let us now take a spherically symmetric metric with the metric functions depending only on r and t,

$$ds^2 = -e^{\nu(t,r)}dt^2 + e^{\lambda(t,r)}dr^2 + r^2(d\theta^2 + \sin^2\theta d\varphi^2)\,. \tag{3.7}$$

Denoting the time derivative by a dot and the radial derivative by a prime, the conservation of the energy-momentum tensor, $T^\nu_{\mu;\nu} = 0$, leads to

$$\dot{T}^0_1 + T^{1'}_1 + \frac{1}{2}T^0_1(\dot{\lambda} + \dot{\nu}) + \frac{1}{2}(T^1_1 - T^0_0)\nu' + \frac{2}{r}(T^1_1 - T^2_2) = 0\,. \tag{3.8}$$

Introducing the dimensionless variables $x = r\mu$ and $\gamma(r) = (8\pi G)^{\frac{1}{2}}\phi(r)$ and taking Einstein's equations for R^0_0 and R^1_1, along with (3.8), we finally get the equations

$$\mu^2 e^\nu\left[\gamma'(x\lambda' - x\nu' - 4) + 2xe^\lambda\gamma - 2x\gamma''\right] - 2x\omega^2 e^\lambda\gamma = 0\,, \tag{3.9}$$

$$\mu^2 e^{-\lambda}(x\lambda' - x^2\gamma'^2 + e^\lambda - 1) + x^2\gamma^2(-\mu^2 - \omega^2 e^\nu) = 0\,, \tag{3.10}$$

and

$$\mu^2 e^{-\lambda}(-x\nu' + x^2\gamma'^2 + e^\lambda - 1) + x^2\gamma^2(-\mu^2 + \omega^2 e^\nu) = 0\,. \tag{3.11}$$

The boundary conditions at the origin read

$$\begin{aligned}\lambda(x) &= \frac{\gamma_0^2 r^2}{3}\left(\frac{\omega^2}{\mu^2}e^{-\nu_0}+1\right)+\mathcal{O}(r^4)\,,\\ \nu(x) &= \nu_0+\frac{\gamma_0^2 r^2}{3}\left(2\frac{\omega^2}{\mu^2}e^{-\nu_0}-1\right)+\mathcal{O}(r^4)\,,\\ \gamma(x) &= \gamma_0-\frac{\gamma_0 r^2}{6}\left(\frac{\omega^2}{\mu^2}e^{-\nu_0}-1\right)+\mathcal{O}(r^4)\,,\end{aligned} \tag{3.12}$$

where γ_0 and ν_0 are constants, while at infinity, the scalar field behaves as

$$\gamma(x) = c_0\frac{e^{-x\sqrt{1-\frac{\omega^2}{\mu^2}}}}{x}+\dots\,, \tag{3.13}$$

where c_0 is a constant. The metric functions e^ν and e^λ behave asymptotically as the Schwarzschild metric with the Schwarzschild mass $m(x)$ approaching a positive constant value which is the ADM mass of the star. Note that $\omega<\mu$, which is a bound state condition.

3.1.3 Numerical results

As a global analytical solution to the equations (3.9)-(3.11) appears to be intractable, a shooting method was implemented for the parameter ω, at each step incrementing the value of γ_0 and making use of the previous solution to find the next.

Figure 3.1 shows a plot of the scalar field γ and the metric functions λ and ν in terms of the rescaled radial coordinate x. It is visible that the field is exponentially supressed at a finite r, so we can consider the star to be confined in a finite region of space[1]. Note that here we are only interested in nodeless solutions, as studies suggest that excited states of scalar boson stars are always unstable [43].

With this choice of variables and ansatz, the total number of particles, (3.6), reads

$$Q = \omega\int dx x^2\sigma^2 e^{\frac{1}{2}(\lambda-\nu)}\,. \tag{3.14}$$

The mass was calculated at infinity taking the spacetime at large distances to be given by the Schwarzschild metric. On Figure 3.2, we plot the ADM mass and the total number of particles of the boson star as a function of the central density γ_0. The inset shows the mass as a function of the fundamental frequency ω. As the central density increases, the mass and particle number rise abruptly until they reach a maximum value of $0.633\ M_{Pl}^2/\mu$ and $0.653\ M_{Pl}^2/\mu^2$, respectively, then M and Q drop to a minimum and oscillate around a positive asymptotic value. It is also visible that $\omega\to 1$ as $\gamma_0\to 0$. It then decreases to a minimum and follows a spiral around a positive value.

The black dot marks the point of maximum mass. Ref. [32] establishes that point as the upper value of linear stability, meaning that solutions with a central density lower than that are linearly stable and those with a higher one are linearly unstable.

[1] As boson stars do not have a hard surface like the one present in neutron stars, their bulk is normally taken to be a large percentage of their mass, e.g. 99%.

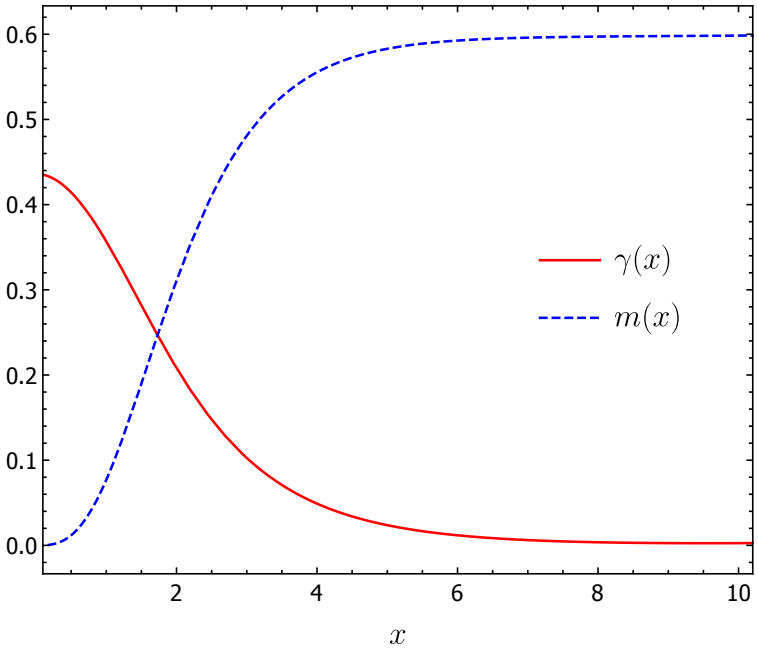

Figure 3.1: Plot of the field γ and the mass m as functions of the radial coordinate for a solution characterized by $\gamma_0 = 0.436$, $\omega = 0.839$ and $M = 0.597\ M_{Pl}^2/\mu$. Here, the Schwarzschild mass is given by $m(x) = x/2(1 - e^{-\lambda})$.

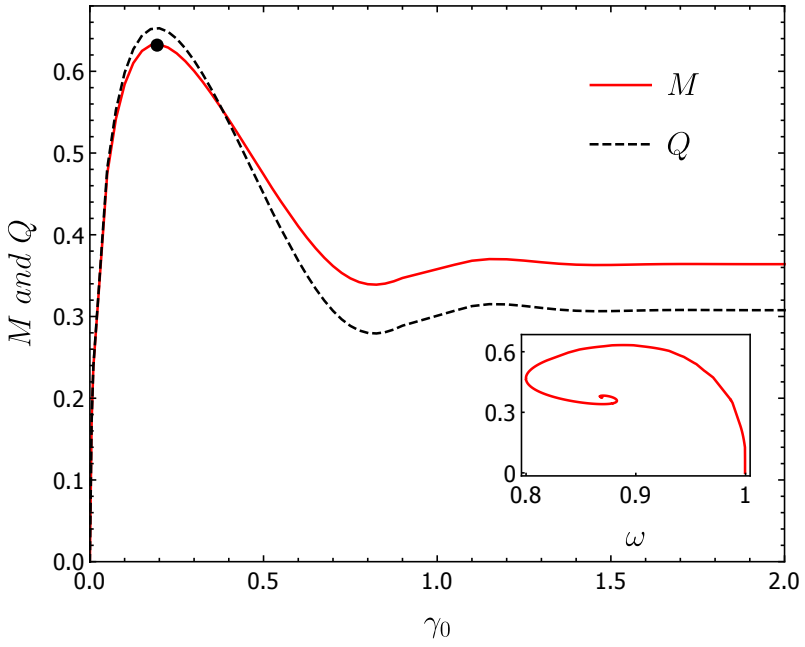

Figure 3.2: ADM mass and total number of particles in terms of the central density for a scalar boson star in an asymptotically flat spacetime. M is given in units of M_{Pl}^2/μ and Q in units of M_{Pl}^2/μ^2. The inset shows the ADM mass as a function of the fundamental frequency.

If one defines the binding energy as $M - Q\mu$, it is clear that it is negative for small values of γ_0 and then becomes positive, pointing towards an excess energy of the solutions with a large central density and suggesting that these are unstable against perturbations.

3.2 Proca stars

The notation used in this section is the one used in Ref. [15], where these structures of non-interacting spin-1 particles were first constructed. Such stars are shown to share various properties with their spinless counterpart.

3.2.1 Framework

The Einstein-(complex)-Proca model is described by the action

$$S = \int d^4\sqrt{-g}\left(\frac{R}{16\pi G} - \frac{1}{4}\mathcal{F}_{\mu\nu}\bar{\mathcal{F}}^{\mu\nu} - \frac{1}{2}\mu^2\mathcal{A}_\mu\bar{\mathcal{A}}^\mu\right) . \tag{3.15}$$

The Einstein and Proca field equations are

$$R_{\mu\nu} - \frac{1}{2}g_{\mu\nu}R = 8\pi G T_{\mu\nu} , \tag{3.16}$$

and

$$\nabla_\mu\mathcal{F}^{\mu\nu} = \mu^2\mathcal{A}^\nu , \tag{3.17}$$

respectively, with an energy-momentum tensor given by

$$T_{\mu\nu} = -\mathcal{F}_{\sigma(\mu}\bar{\mathcal{F}}^{\sigma}_{\nu)} - \frac{1}{4}g_{\mu\nu}\mathcal{F}_{\alpha\beta}\bar{\mathcal{F}}^{\alpha\beta} + \mu^2\left[\mathcal{A}_{(\mu}\bar{\mathcal{A}}_{\nu)} - \frac{1}{2}g_{\mu\nu}\mathcal{A}_\alpha\bar{\mathcal{A}}^\alpha\right] , \tag{3.18}$$

and $\mathcal{F}$ defined as $\mathcal{F} \equiv d\mathcal{A}$. The action (3.15) is invariant under a global $U(1)$ symmetry of the form $\mathcal{A}_\mu \to e^{i\alpha}\mathcal{A}_\mu$, which implies the existence of a conserved 4-current

$$j^\mu = \frac{i}{2}\left(\bar{\mathcal{F}}^{\mu\nu}\mathcal{A}_\nu - \mathcal{F}^{\mu\nu}\bar{\mathcal{A}}_\nu\right) . \tag{3.19}$$

This, in turn, implies the existence of a conserved Noether charge Q, once again the particle number, given by (3.6).

3.2.2 Equations of motion and boundary conditions

Considering only spherically symmetric solutions, we can write the metric as

$$ds^2 = -\sigma^2(r)N(r)dt^2 + \frac{1}{N(r)}dr^2 + r^2(d\theta^2 + \sin^2\theta d\varphi^2) , \tag{3.20}$$

with $N(r) = 1 - 2m(r)/r$ and the Proca potential as

$$\mathcal{A} = e^{-i\omega t}\left[f(r)dt + ig(r)dr\right] , \tag{3.21}$$

where $f(r)$, $g(r)$ are real functions of the radial coordinate[2]. The Proca equations are

$$\left[\frac{r^2(f'-\omega g)}{\sigma}\right]' = \frac{\mu^2 r^2 f}{\sigma N}\,, \tag{3.22}$$

and

$$\omega g - f' = \frac{\mu^2\sigma^2 N g}{\omega}\,, \tag{3.23}$$

while Einstein's equations, namely those for G_{00} and $\frac{2}{N}G_{00} + 2N\sigma^2 G_{11}$, yield

$$m' = 4\pi G r^2\left[\frac{(f'-\omega g)^2}{2\sigma^2} + \frac{1}{2}\mu^2\left(g^2 N + \frac{f^2}{N\sigma^2}\right)\right]\,, \tag{3.24}$$

and

$$\sigma' = 4\pi G r\mu^2\sigma\left(g^2 + \frac{f^2}{N^2\sigma^2}\right)\,. \tag{3.25}$$

The behaviour of equations (3.22)-(3.25) near the origin is the following:

$$\begin{aligned} f(r) &= f_0 + \frac{f_0}{6}r^2\left(\mu^2 - \frac{\omega^2}{\sigma_0^2}\right) + \mathcal{O}(r^4)\,,\\ g(r) &= -\frac{f_0\omega}{3\sigma_0^2}r + \mathcal{O}(r^3)\,,\\ m(r) &= \frac{4\pi G f_0^2\mu^2}{6\sigma_0^2}r^3 + \mathcal{O}(r^5)\,,\\ \sigma(r) &= \sigma_0 + \frac{4\pi G f_0^2\mu^2}{2\sigma_0}r^2 + \mathcal{O}(r^4)\,, \end{aligned} \tag{3.26}$$

where f_0 and σ_0 are constants. At spatial infinity, the different quantities behave thusly:

$$\begin{aligned} f(r) &= c_0\frac{e^{-r\sqrt{\mu^2-\omega^2}}}{r} + \dots\,,\\ g(r) &= c_0\frac{\omega}{\sqrt{\mu^2-\omega^2}}\frac{e^{-r\sqrt{\mu^2-\omega^2}}}{r} + \dots\,,\\ m(r) &= M + \dots\,,\\ \log\sigma(r) &= -4\pi G\frac{c_0\mu^2}{2(\mu^2-\omega^2)^{3/2}}\frac{e^{-2r\sqrt{\mu^2-\omega^2}}}{r} + \dots\,, \end{aligned} \tag{3.27}$$

where M is the ADM mass and c_0 is a constant.

3.2.3 Numerical results

In the following, the constants are set to $\mu = 1$ and $4\pi G = 1$ by changing $r \to r\mu$, $m \to m\mu$, $\omega \to \omega\mu$, $f \to f\sqrt{4\pi G}$ and $g \to g\sqrt{4\pi G}$. Eq.(3.6), in this case, gives

$$Q = \frac{1}{\omega}\int dr\frac{r^2 g^2\sigma}{N}\,. \tag{3.28}$$

A method similar to the one used for scalar boson stars was used to solve the system (3.22)-(3.25)

[2]Note that a complex Proca field can be thought of as two independent real fields of mass μ.

numerically. Figure 3.3 shows a plot of the field components, f and g, and the metric functions, σ and m, in terms of r. Note that both components of the field are exponentially supressed at some r and that both σ and m approach constant positive values. Also, in the family of solutions presented here, f has one node (hardly noticeable on Figure 3.3) and g is nodeless.

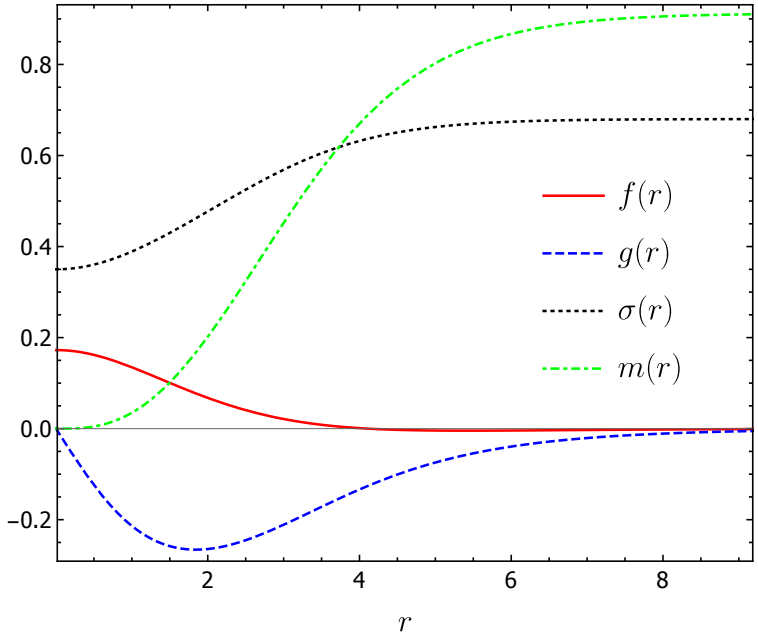

Figure 3.3: Plot of the field components, f and g, and the metric functions, σ and m, in terms of the radial coordinate for a solution described by $f_0 = 0.176$, $\omega = 0.858$ and $M = 1.052\ M_{Pl}^2/\mu$.

On Figure 3.4 the ADM mass and the total particle number are plotted against f_0 and against the fundamental frequency ω. It is visible that the solutions do not change qualitatively when one considers spin-1 particles instead of scalar ones. Nevertheless, the maximum mass and particle number reached by the star are larger than those for a regular boson star, namely $1.058\ M_{Pl}^2/\mu$ and $1.087\ M_{Pl}^2/\mu^2$, respectively. Once again, the black dot marks the point of maximum mass as well as the upper value of stability, as asserted in [15]. This calculation is performed in detail on chapter 6.

Similarly to the scalar case, looking at Figure 3.4, one can argue that solutions above a certain value of f_0 have excess energy and are unstable against perturbations.

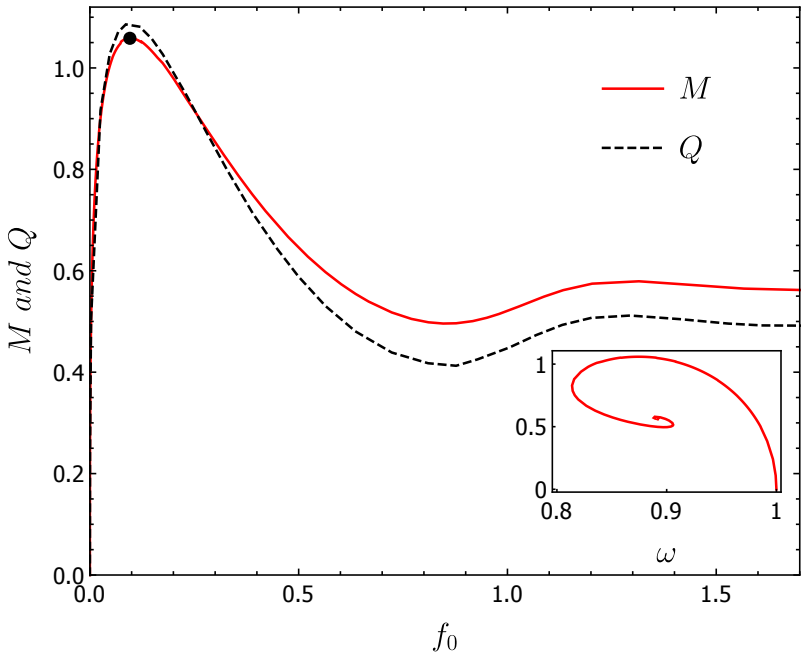

Figure 3.4: ADM mass and total particle number in terms of f_0 for a Proca star in an asymptotically flat spacetime, in units of M_{Pl}^2/μ and M_{Pl}^2/μ^2, respectively. The inset shows the ADM mass as a function of the fundamental frequency.

Chapter 4

Numerical solutions in AdS

A procedure analogous to the one used in the previous chapter is employed here in order to obtain the ADM mass and total particle number of scalar boson stars and Proca stars in asymptotically AdS spacetimes.

4.1 Scalar boson stars

The following calculations make use of the notation and ansatz present in Ref. [42]. This paper shows a detailed numerical study of scalar boson star solutions in AdS for different values of the cosmological constant.

4.1.1 Framework

The action for a scalar boson star in AdS is the following:

$$S = -\int d^4\sqrt{-g}\left(\frac{R-2\Lambda}{16\pi G} - g^{\mu\nu}\Phi^*_{,\mu}\Phi_{,\nu} - \mu^2|\Phi|^2\right) . \tag{4.1}$$

In this case, Einstein's equations take the form

$$R_{\mu\nu} - \frac{1}{2}g_{\mu\nu}R + \Lambda g_{\mu\nu} = 8\pi G T_{\mu\nu} . \tag{4.2}$$

with an energy-momentum tensor given by

$$T_{\mu\nu} = \Phi^*_{,\mu}\Phi_{,\nu} + \Phi^*_{,\nu}\Phi_{,\mu} - g_{\mu\nu}(g^{\alpha\beta}\Phi^*_{,\alpha}\Phi_{,\beta} + \mu^2|\Phi|^2) . \tag{4.3}$$

Once again, we take the field to be given by $\Phi(t,r) = \phi(r)e^{-i\omega t}$ and the metric to be

$$ds^2 = -e^{-2\delta(r)}F(r)dt^2 + \frac{1}{F(r)}dr^2 + r^2(d\theta^2 + \sin^2\theta d\varphi^2) , \tag{4.4}$$

with $F(r) = 1 - 2m(r) - \Lambda r^2/3$.

4.1.2 Equations of motion and boundary conditions

Einstein's equations yield

$$m' = 4\pi G r^2 \left[F\phi'^2 + \mu^2\phi^2 + \frac{e^{2\delta}}{F}\omega^2\phi^2 \right] , \tag{4.5}$$

and

$$(e^{-\delta})' = 8\pi G r \left[\frac{\omega^2 e^{\delta}\phi^2}{F^2} + \phi'^2 e^{-\delta} \right] , \tag{4.6}$$

while the Klein-Gordon equation for curved spacetime gives

$$(r^2 e^{-\delta} F\phi')' = r^2\phi e^{-\delta}\left(\mu^2 + \omega^2 \frac{e^{2\delta}}{F} \right) . \tag{4.7}$$

Near the origin, the relevant quantities of the system were found to behave in the following way:

$$\begin{aligned} \phi(r) &= \phi_0 + r^2 \frac{\phi_0(1 - e^{2\delta_0})}{6} + \mathcal{O}(r^4) , \\ m(r) &= r^3 \frac{\phi_0^2(1 + e^{2\delta_0})}{6} + \mathcal{O}(r^5) , \\ \delta(r) &= \delta_0 - \frac{1}{2} e^{2\delta_0}\phi_0^2 r^2 + \mathcal{O}(r^4) , \end{aligned} \tag{4.8}$$

while at spatial infinity, they behave like

$$\begin{aligned} \phi(r) &= c_0 r^a + \dots , \\ m(r) &= M + \dots , \\ e^{-\delta(r)} &= 1 + \frac{a c_0^2}{2} r^{2a} + \dots , \end{aligned} \tag{4.9}$$

where c_0 is a constant and $a = -3/2 - \sqrt{9/4 - 1/\Lambda}$. We see here the complicated power decay that does not take place when $\Lambda = 0$ (see (3.13)).

4.1.3 Numerical results

This choice of variables and ansatz in (3.6) leads to

$$Q = 2\omega \int dr \frac{r^2\phi^2 e^{\delta}}{F} . \tag{4.10}$$

The system (4.5)-(4.7) was integrated numerically in order to obtain Figure 4.1, a profile of the ADM mass and particle number in terms of the central density for $\Lambda = 0$, $\Lambda = -0.05\mu^2$ and $\Lambda = -\mu^2$. The same results were used to plot the mass in terms of the fundamental frequency for the three values of the cosmological constant, shown on Figure 4.2.

The maximum mass for $\Lambda = 0$ is, once again, $0.633\ M_{Pl}^2/\mu$, for $\Lambda = -0.05\mu^2$ it is $0.480\ M_{Pl}^2/\mu$ and for $\Lambda = -\mu^2$ it is $0.239\ M_{Pl}^2/\mu$. The maximum particle numbers are, respectively, $0.653\ M_{Pl}^2/\mu^2$, $0.436\ M_{Pl}^2/\mu^2$ and $0.121\ M_{Pl}^2/\mu^2$. So we see that, although the qualitative behaviour of the solutions is not affected by the introduction of a negative consmological constant, the maximum mass and particle

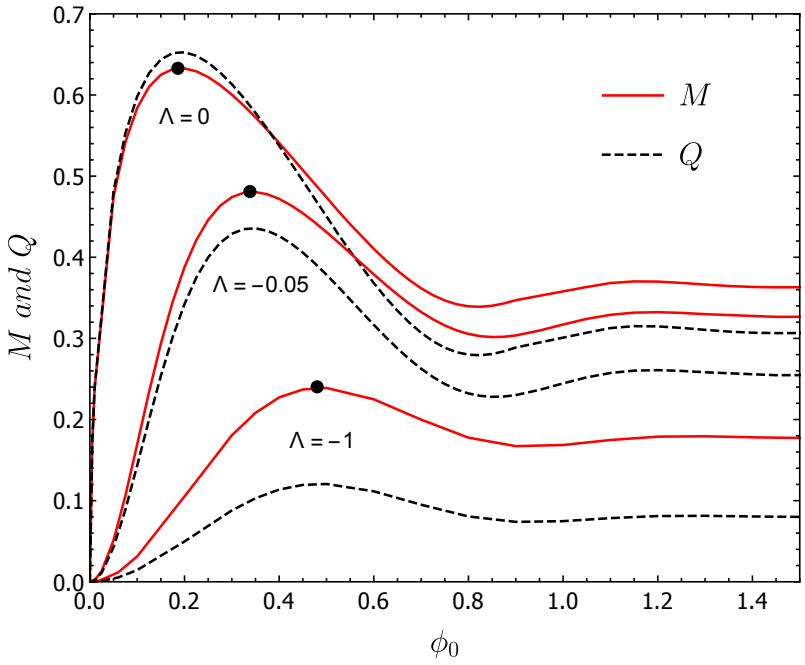

Figure 4.1: ADM mass and number of particles in terms of the central density for a scalar boson star in AdS. The mass is given in units of M_{Pl}^2/μ, the number of particles in units of M_{Pl}^2/μ^2 and Λ in units of μ^2.

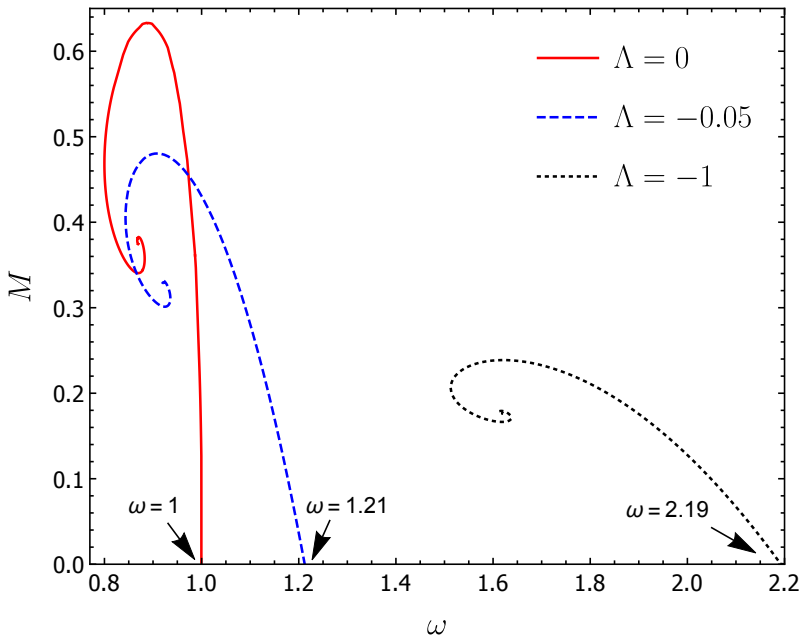

Figure 4.2: ADM mass in terms of the fundamental frequency for a scalar boson star in AdS. The mass is in units of M_{Pl}^2/μ and Λ in units of μ^2.

number decreases. Also, the central density at which that maximum occurs shifts towards higher values with a decreasing Λ.

Ref. [42] establishes that the point of maximum mass corresponds to the upper value of linear stability (black dot on Figure 4.1), just as in asymptotically flat spacetime. In AdS, the binding energy does not hold the same meaning as in asymptotically flat spacetimes given the confining nature of this spacetime.

A configuration with excess energy would presumably radiate and decay away, but the radiation would just reach the boundary of the spacetime and come back in a finite time interval. Therefore, using the positivity of the binding energy to suggest an instability of self-gravitating structures in AdS seems to be invalid. In fact, both linearly and non-linearly stable solutions have been found in this spacetime [42, 21, 22, 23, 24, 25].

It is worth mentioning that it is possible to find similar solutions with $\mu = 0$ in AdS (see Ref. [24]), although these do not exist in asymptotically flat spacetimes. This discrepancy is due to the fact that the boundary of the AdS spacetime is in causal contact with its interior. It thus acts as a natural box and scalar boson stars behave as stationary waves inside that box.

4.2 Proca stars

There is still no work in the literature concerning self-gravitating structures of spin-1 particles in asymptotically AdS spacetimes. These solutions are constructed here and it is seen that increasing the modulus of the negative cosmological constant changes their behaviour in a similar way as it does for scalar boson stars.

We established a no-hair theorem for Proca stars in AdS stating that spherically symmetric gravitational collapse always ends in the Schwarzschild-AdS metric. The proof of this theorem can be easily generalized from the one in asymptotically flat spacetime in Ref. [40] and it is presented in Appendix B.

4.2.1 Framework

Taking the action

$$S = \int d^4\sqrt{-g}\left(\frac{R-2\Lambda}{16\pi G} - \frac{1}{4}\mathcal{F}_{\mu\nu}\bar{\mathcal{F}}^{\mu\nu} - \frac{1}{2}\mu^2\mathcal{A}_\mu\bar{\mathcal{A}}^\mu\right), \tag{4.11}$$

we retrieve equations (3.17) and (4.2) with an energy-momentum tensor given by (3.18).

Let us now take the metric to be

$$ds^2 = -\sigma^2(r)F(r)dt^2 + \frac{1}{F(r)}dr^2 + r^2(d\theta^2 + \sin^2\theta d\varphi^2), \tag{4.12}$$

with $F(r)$ defined as before, and the Proca potential written as (3.21).

4.2.2 Equations of motion and boundary conditions

Einstein's equations and Proca equations yield

$$\left[\frac{r^2(f'-\omega g)}{\sigma}\right]' = \frac{\mu^2 r^2 f}{\sigma F}, \tag{4.13}$$

$$\omega g - f' = \frac{\mu^2\sigma^2 F g}{\omega}, \tag{4.14}$$

$$m' = 4\pi G r^2\left[\frac{(f'-\omega g)^2}{2\sigma^2} + \frac{1}{2}\mu^2\left(g^2F + \frac{f^2}{F\sigma^2}\right)\right], \tag{4.15}$$

and

$$\sigma' = 4\pi G r \mu^2 \sigma \left(g^2 + \frac{f^2}{F^2 \sigma^2} \right) . \tag{4.16}$$

The boundary conditions at the origin are (3.26), while at spatial infinity, the following behaviour is found:

$$\begin{aligned} f(r) &= c_0 r^{\alpha} \dots , \\ g(r) &= -\frac{c_0 l^4 \omega}{\alpha + 1} r^{\alpha - 3} + \dots , \\ m(r) &= M + 4\pi G c_0^2 \frac{\alpha^2 + \mu^2 l^2}{2(1 + 2\alpha)} r^{2\alpha + 1} + \dots , \\ \log \sigma(r) &= 4\pi G c_0^2 \frac{\mu^2 l^4}{2(\alpha - 1)} r^{2\alpha - 2} + \dots , \end{aligned} \tag{4.17}$$

where c_0 is a constant, M is the ADM mass, $l^2 = -3/\Lambda$ is the AdS curvature radius squared and $\alpha = -(\sqrt{1 + 4\mu^2 l^2} + 1)/2$.

4.2.3 Numerical results

The expression for the total number of particles is, in this case,

$$Q = \frac{1}{\omega} \int dr \frac{r^2 g^2 \sigma}{F} . \tag{4.18}$$

The field equations were solved numerically using the same method as before. On Figure 4.3 the ADM mass and total particle number are plotted against f_0 and on Figure 4.4 the ADM mass is plotted against the fundamental frequency for $\Lambda = 0$, $\Lambda = -0.05\mu^2$ and $\Lambda = -\mu^2$.

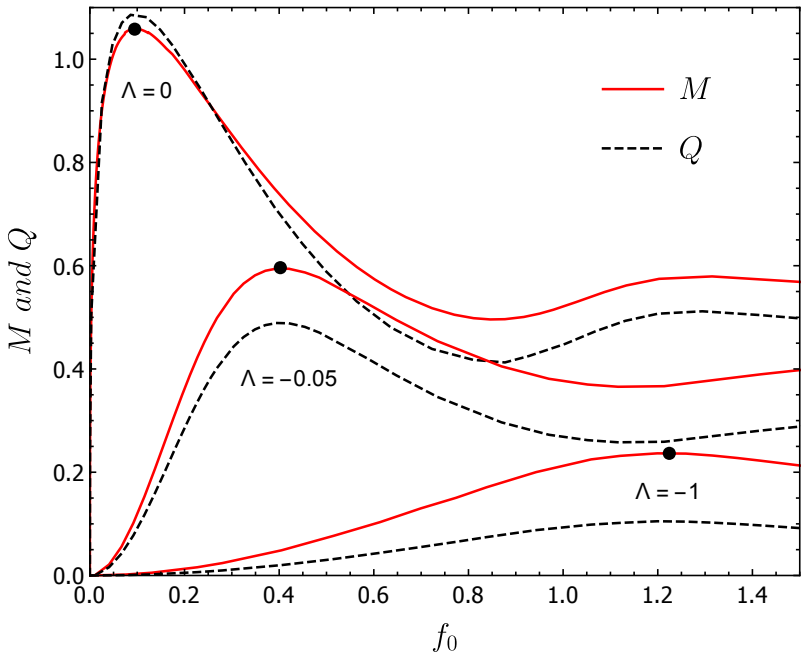

Figure 4.3: ADM mass and number of particles in terms of f_0 for a Proca star in AdS. The mass is given in units of M_{Pl}^2/μ, the number of particles in units of M_{Pl}^2/μ^2 and Λ in units of μ^2.

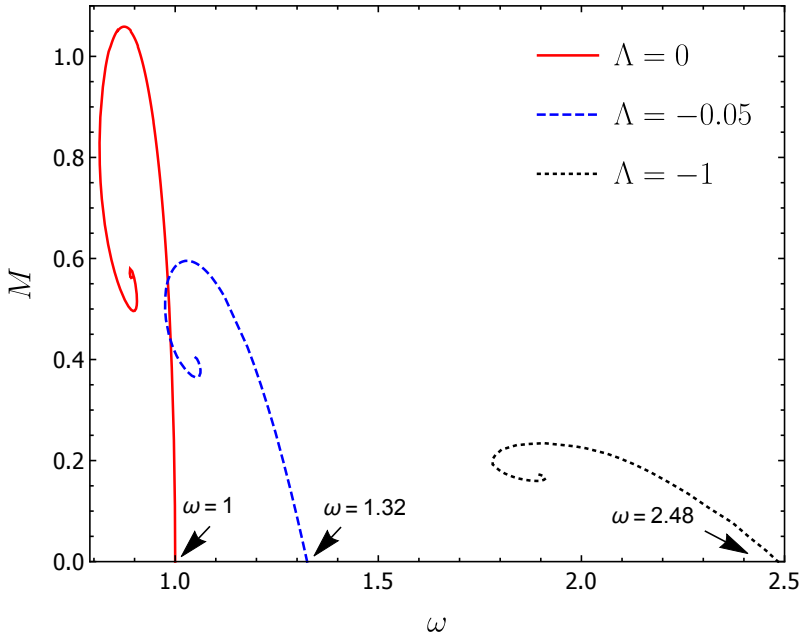

Figure 4.4: ADM mass in terms of the fundamental frequency for a Proca star in AdS. The mass is in units of M_{Pl}^2/μ and Λ in units of μ^2.

The maximum mass for $\Lambda = 0$ is, once again, $1.058\ M_{Pl}^2/\mu$, for $\Lambda = -0.05\mu^2$ it is $0.595\ M_{Pl}^2/\mu$ and for $\Lambda = -\mu^2$ it is $0.237\ M_{Pl}^2/\mu$ (black dots on Figure 4.3). The maximum particle numbers are, respectively, $1.087\ M_{Pl}^2/\mu^2$, $0.489\ M_{Pl}^2/\mu^2$ and $0.105\ M_{Pl}^2/\mu^2$. As expected, the introduction of a negative cosmological constant preserves the qualitative behaviour of the solutions, once again decreasing the maximum mass and shifting the value of f_0 at which it occurs towards higher values.

An interesting contrast between Proca stars and scalar ones is that spin-1 solutions do not exist for $\mu = 0$. This can be understood if we, once again, take AdS spacetime to work as a box. It is known that Maxwell fields do not allow for spherically symmetric stationary everywhere regular waves and hence, Proca stars of massless bosons cannot exist for any value of Λ.

4.3 Proca stars in five dimensions

Ref. [42] shows stark differences in the behaviour of scalar boson stars in four and five-dimensional AdS spacetimes. This makes it interesting to find solutions of Proca stars in five dimensions and see whether these behave in a similar manner. Here we construct such solutions numerically and argue an instability against perturbations in the asymptotically flat case.

4.3.1 Framework

In five dimensions, the spherically symmetric metric becomes

$$ds^2 = \sigma^2(r)F_{5D}(r)dt^2 + \frac{1}{F_{5D}(r)}dr^2 + r^2 d\Omega_3^2\,, \tag{4.19}$$

where $d\Omega_3^2$ denotes the three-dimensional unit sphere line element and the function $F_{5D}(r)$ is given by

$$F_{5D}(r) = 1 - \frac{2m(r)}{r^2} - \frac{\Lambda r^2}{6}\,. \tag{4.20}$$

4.3.2 Equations of motion and boundary conditions

Einstein's equations, together with the Proca field equations, yield the following system of ordinary differential equations:

$$\left[\frac{r^2(f'-\omega g)}{\sigma}\right]' + \frac{r}{\sigma}(f'-\omega g) = \frac{\mu^2 r^2 f}{\sigma F_{5D}}\,, \tag{4.21}$$

$$\omega g - f' = \frac{\mu^2\sigma^2 F_{5D} g}{\omega}\,, \tag{4.22}$$

$$m' = 4\pi G r^3\left[\frac{(f'-\omega g)^2}{3\sigma^2} + \frac{1}{3}\mu^2\left(g^2 F_{5D} + \frac{f^2}{F_{5D}\sigma^2}\right)\right]\,, \tag{4.23}$$

and

$$\sigma' = \frac{8}{3}\pi G r \mu^2 \sigma\left(g^2 + \frac{f^2}{F_{5D}^2\sigma^2}\right)\,. \tag{4.24}$$

The boundary conditions at the origin imposed by (4.21)-(4.24) are

$$\begin{aligned}
f(r) &= f_0 + \frac{f_0}{8}r^2\left(\mu^2 - \frac{\omega^2}{\sigma_0^2}\right) + \mathcal{O}(r^4)\,,\\
g(r) &= -\frac{f_0\omega}{4\sigma_0^2}r + \mathcal{O}(r^3)\,,\\
m(r) &= \frac{4\pi G f_0^2\mu^2}{12\sigma_0^2}r^4 + \mathcal{O}(r^6)\,,\\
\sigma(r) &= \sigma_0 + \frac{4\pi G f_0^2\mu^2}{3\sigma_0}r^2 + \mathcal{O}(r^4)\,,
\end{aligned} \tag{4.25}$$

where f_0 and σ_0 are constants. The boundary conditions at spatial infinity in AdS and flat asymptotics are ommited here as they are similar to (4.17) and (3.27), respectively.

4.3.3 Numerical Results

Equation (3.6) in five dimensions gives

$$Q = \frac{\pi}{2\omega}\int_0^\infty r^3 g^2 \sigma F_{5D} dr\,. \tag{4.26}$$

The main difference between the four and five-dimensional cases occurs when $\Lambda = 0$. Unlike the four-dimensional case, in the limit $f_0 \to 0$, the mass and charge of the solutions are finite. This is shown on Fig. 4.5, which shows a plot of the ADM mass and charge of the five-dimensional solutions for $\Lambda = 0$ and $\Lambda = -0.05\mu^2$. This behavior was also noticed for scalar boson stars in Refs. [44, 45] and it is present uniquely in asymptotically flat solutions. For $\Lambda \neq 0$ the behavior is analogous to the one found in four dimensions, as shown in Fig. 4.5.

Taking the asymptotically flat case, it is visible that the particle number is smaller than the ADM mass

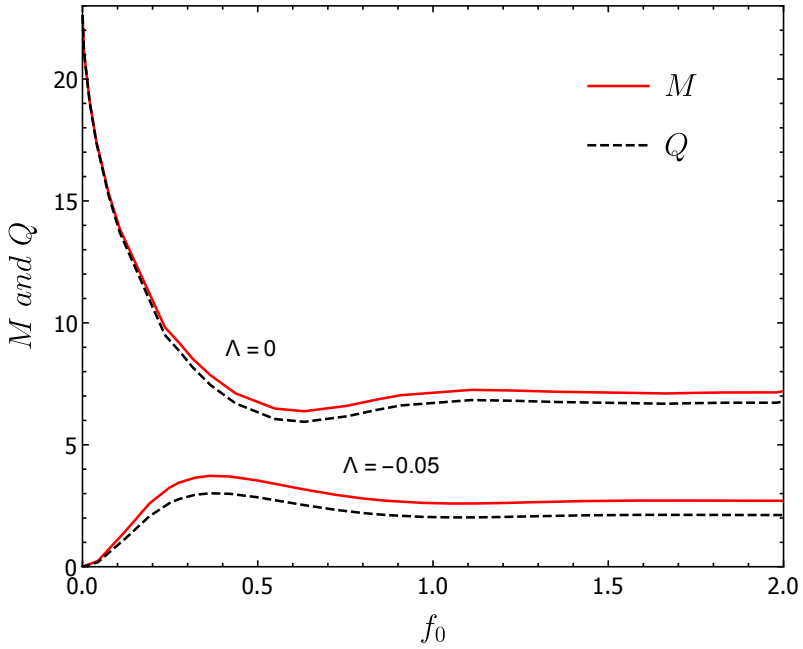

Figure 4.5: ADM mass and particle number in terms of f_0 for a Proca star in five dimensions. The mass is given in units of M_{Pl}^3/μ^2, the number of particles in units of M_{Pl}^3/μ^3 and Λ in units of μ^2.

for all solutions. If we take the binding energy to be given by $M - Q\mu$, then it is always positive, pointing towards an excess energy in the solutions and thus suggesting that every solution is unstable against perturbations.

Similarly to the scalar case, for Proca star solutions in five-dimensional AdS, both M and Q vanish when $f_0 \to 0$, while there is a maximum mass and charge at a finite value of f_0. This suggests a stable set of solutions in AdS. Unfortunately, due to the greater complexity of the five-dimensional solutions, we could not confirm this supposition through a linear stability analysis and we leave a more complete study for future work.

The maximum mass for $\Lambda = -0.05\mu^2$ is $3.728\ M_{Pl}^3/\mu^3$, while the maximum particle number is $3.012\ M_{Pl}^3/\mu^2$.

Chapter 5

Analytical solutions in AdS

It is possible to obtain solutions of boson stars analytically if we consider a perturbative expansion in the amplitude of the fields. Such solutions are the normal modes of the fields. For this purpose, let us introduce the vacuum AdS metric in global coordinates:

$$ds^2 = -\left(\frac{r^2}{l^2}+1\right)dt^2 + \frac{dr^2}{\left(\frac{r^2}{l^2}+1\right)} + r^2 d\Omega_2^2\,, \tag{5.1}$$

where $l^2 = -3/\Lambda$. As the field is taken to be a perturbation, the Schwarzschild mass $m(r)$ vanishes. Using this approximation, one can obtain values for the fundamental frequency, the total mass of the star and its number of particles, in order to compare them with the ones obtained numerically. This allows for the validation of the numerical method and a corroboration of the values obtained thusly.

5.1 Scalar boson stars

We start by considering the following expansion:

$$\begin{aligned} \phi(r) &= \epsilon\frac{\psi(r)}{r} + \mathcal{O}(\epsilon^3)\,, \\ m(r) &= \epsilon^2 m_2(r) + \mathcal{O}(\epsilon^4)\,, \\ e^{-\delta(r)} &= 1 + \epsilon^2\delta_2(r) + \mathcal{O}(\epsilon^4)\,, \end{aligned} \tag{5.2}$$

where $F_0(r) = 1 + \frac{r^2}{l^2}$ and ϵ is a small parameter, which can be chosen to be the free-parameter $\phi_0 \equiv \phi(r=0) = \epsilon$, by normalizing the function ψ as

$$\left.\frac{\psi}{r}\right|_{r\to 0} = 1\,. \tag{5.3}$$

At linear order in ϵ, the problem reduces to solving the field equations in an AdS background. The spherically symmetric Klein-Gordon equation is

$$F_0^2\frac{d^2\psi}{dr^2} + F_0' F_0\frac{d\psi}{dr} + \left[\omega^2 - F_0\left(\frac{2}{l^2}+\mu^2\right)\right]\psi = 0\,. \tag{5.4}$$

We define the tortoise coordinate r_* as

$$\frac{\partial r}{\partial r_*} = F_0(r)\,, \tag{5.5}$$

and use it to write (5.4) as

$$\frac{d^2\psi}{dr_*^2} + \left[\omega^2 - F_0\left(\frac{2}{l^2} + \mu^2\right)\right]\psi = 0\,. \tag{5.6}$$

Now, making use of the variable $x \equiv \sin^2(r_*/l)$, we get the equation

$$\frac{\partial^2\psi}{\partial x^2} + \frac{\tau}{\eta}\frac{\partial\psi}{\partial x} + \frac{\zeta}{\sigma^2}\psi = 0\,, \tag{5.7}$$

where τ, η and ζ are given by

$$\begin{aligned}\tau &= 4\omega^2 l^2 x(1-x) - 4x(2+\mu^2 l^2)\,,\\ \eta &= 4x(1-x)\,,\\ \zeta &= 2(1-2x)\,.\end{aligned} \tag{5.8}$$

Finally, making

$$\psi(x) = Z(x)(1-x)^{\frac{1}{2}(k_s-1)}\sqrt{x}\,, \tag{5.9}$$

with $k_s = 3/2 + \sqrt{9/4 + \mu^2 l^2}$, we get a hypergeometric differential equation for $Z(x)$ in the standard form:

$$x(1-x)\frac{d^2Z}{dx^2} + [c - (a+b+1)x]\frac{dZ}{dx} - (ab)Z = 0\,, \tag{5.10}$$

where $a = (k_s - l\omega)/2$, $b = (k_s + l\omega)/2$ and $c = 3/2$. The most general solution to this equation is given by

$$Z(x) = A\,{}_2F_1\left(a, b; c; x\right) + Bx^{1-c}\,{}_2F_1\left(1+a-c, 1+b-c; 2-c; x\right)\,. \tag{5.11}$$

Requiring a regular solution at the origin $r = 0$, implies that $B = 0$, while imposing regularity of the solution at infinity gives the spectrum:

$$\omega l = k_s + 2n\,. \tag{5.12}$$

where n parametrizes the excitation level of the boson star.

Let us now compare this result with the numerical frequencies. For $n = 0$, we get a fundamental frequency of $\omega \approx 2.19$ with a cosmological constant of $-\mu^2$ and $\omega \approx 1.21$ with a cosmological constant of $-0.05\mu^2$. Looking at Figure 4.2 we see that, in the approximation of a small central density (lower part of the curve) the values of the frequency correspond with good accuracy to those given by (5.12).

In order to compare this result with the mass-central density curve, one can consider higher order corrections in $m(r)$. In particular, the ADM mass of the solutions can be obtained by taking into account second order terms in ϵ and integrating equation (4.5) to obtain

$$M = 4\pi\int \rho r^2 dr\,. \tag{5.13}$$

Considering $\rho = -T_t^t$, for the fundamental solution $n = 0$, we get

$$M/l = \epsilon^2 \frac{\sqrt{\pi}(k^2 - l^2)\Gamma\left[k - \frac{3}{2}\right]}{4\Gamma[k]}\,, \tag{5.14}$$

while the charge can be obtained from (4.10):

$$Q/l^2 = \epsilon^2 \frac{\sqrt{\pi}(k^2 - l^2)\Gamma\left[k - \frac{3}{2}\right]}{4k\Gamma[k]}\,. \tag{5.15}$$

It is worth noting that, for any n,

$$M = \omega\, Q\,, \tag{5.16}$$

with ω given by eq. (5.12).

On Figure 5.1 we plot (5.14) and (5.15) along with the numerical points in the small field approximation for $\Lambda = -\mu^2$ (Figure 4.1). It is visible that the analytical curve is in agreement with the fully non-linear

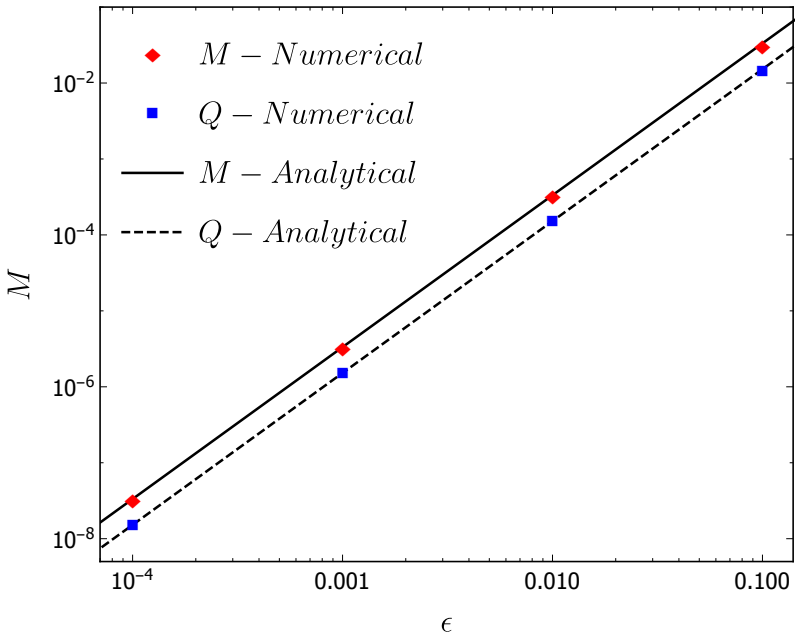

Figure 5.1: Comparison between the perturbative approximations for the mass (5.14) and charge (5.15) and the fully non-linear results of a scalar boson star, as a function of the central density for $\Lambda = -\mu^2$.

results, thus corroborating the numerical method.

5.2 Proca stars

Once again, expanding the relevant functions in powers of ϵ gives

$$
\begin{aligned}
f(r) &= \epsilon \frac{u_1(r)}{r} + \mathcal{O}(\epsilon^3)\,, \\
g(r) &= \epsilon \frac{u_2(r)}{r F_0(r)} + \mathcal{O}(\epsilon^3)\,, \\
m(r) &= \epsilon^2 m_2(r) + \mathcal{O}(\epsilon^4)\,, \\
\sigma(r) &= 1 + \epsilon^2 \sigma_2(r) + \mathcal{O}(\epsilon^4)\,,
\end{aligned}
$$

and we make $f_0 \equiv f(r=0) = \epsilon$ by normalizing the function u_1 as

$$
\left.\frac{u_1}{r}\right|_{r\to 0} = 1\,. \tag{5.17}
$$

The Lorenz condition $\nabla_\alpha A^\alpha = 0$ yields

$$
u_1 = -\frac{F_0 \partial_r (r\, u_2)}{\omega r}\,, \tag{5.18}
$$

which gives, together with the (r) component of the Proca equations,

$$
\frac{d^2 u_2}{dr_*^2} + \left[\omega^2 - F_0\left(\frac{2}{r^2} + \mu^2\right)\right] u_2 = 0\,, \tag{5.19}
$$

where the tortoise coordinate r_* is defined in (5.5). Once again, making use of $x \equiv \sin^2(r_*/l)$, one can define the function $Z(x)$ as

$$
u_2(x) = Z(x)(1-x)^{\frac{1}{2}(3-k_v)} x\,, \tag{5.20}
$$

this time with $k_v = 5/2 + \sqrt{1/4 + \mu^2 l^2}$, in order to get a hypergeometric equation in $Z(x)$, (5.10), where $a = (5 - k - l\omega)/2$, $b = (5 - k + l\omega)/2$ and $c = 5/2$. Requiring well-behaved fields everywhere, we get the frequency spectrum

$$
\omega l = k_v + 2n\,. \tag{5.21}
$$

For $n = 0$, the fundamental frequency is $\omega \approx 2.48$ with $\Lambda = -\mu^2$ and $\omega \approx 1.32$ with $\Lambda = -0.05\mu^2$. Figure 4.4, in the small amplitude approximation, shows that the values of the frequency correspond with good accuracy to those obtained from (5.21).

For $n = 0$, the expressions for the ADM mass and total number of particles in the small amplitude approximation are, respectively,

$$
M/l = \epsilon^2 \frac{\sqrt{\pi} k(k-3)(k-2)\Gamma\left[k - \frac{3}{2}\right]}{24\Gamma[k]}\,, \tag{5.22}
$$

$$
Q/l^2 = \epsilon^2 \frac{\sqrt{\pi} (k-3)(k-2)\Gamma\left[k - \frac{3}{2}\right]}{24\Gamma[k]}\,. \tag{5.23}
$$

Note that (5.16) still holds.

On Figure 5.2 we plot (5.22) and (5.23) with the numerical data in the considered limit for $\Lambda = -\mu^2$ (Figure 4.3), where we see that numerical and analytical results agree, once more, in the small f_0 approximation.

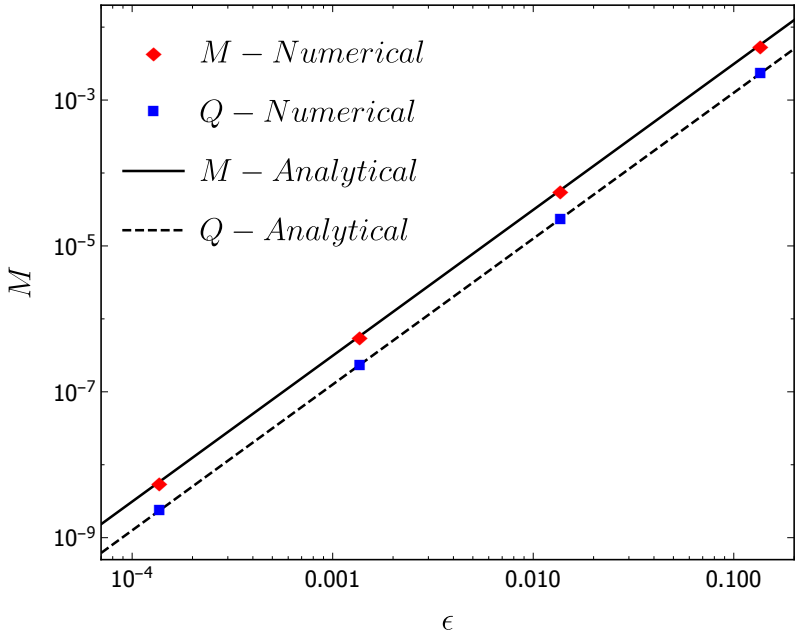

Figure 5.2: Comparison between the perturbative approximations for the mass (5.22) and charge (5.23) and the fully non-linear results of a Proca star, as a function of f_0 for $\Lambda = -\mu^2$.

Chapter 6

Linear stability of Proca stars

Having seen that it is possible to construct Proca star solutions in asymptotically AdS spacetimes we now study the stability of these solutions against small perturbations. We consider linear perturbations around the ground state of spherically symmetric Proca stars, assuming that all perturbations have a harmonic time dependence of the form $e^{-i\Omega t}$, with Ω the characteristic vibrational frequencies. Ref. [15] shows that Proca stars with flat asymptotics are linearly stable from $f_0 \to 0$ until the point of maximum mass, while the same result had formerly been shown for scalar boson stars in both spacetimes [32, 42]. An analogous study for Proca stars in AdS has not yet been shown.

6.1 Equations of motion and boundary conditions

Following [15], the perturbed metric can be written as

$$ds^2 = -\sigma^2(r)F(r)[1 - H_0(r)e^{-i\Omega t}]dt^2 + \frac{[1 + H_2(r)e^{-i\Omega t}]}{F(r)}dr^2 + r^2 d\Omega^2 \,, \tag{6.1}$$

where H_0 and H_2 are small radial perturbations around the background metric and $F(r) = 1 - 2m(r) - \Lambda r^2/3$. The perturbed vector field is written as

$$\begin{aligned} \mathcal{A} &= e^{-i\omega t}\left[\left(f(r) + e^{-i\Omega t}\frac{f_1(r) + if_2(r)}{r}\right)dt + \left(ig(r) + e^{-i\Omega t}\frac{g_1(r) + ig_2(r)}{r}\right)dr\right] , \\ \bar{\mathcal{A}} &= e^{i\omega t}\left[\left(f(r) + e^{-i\Omega t}\frac{f_1(r) - if_2(r)}{r}\right)dt + \left(-ig(r) + e^{-i\Omega t}\frac{g_1(r) - ig_2(r)}{r}\right)dr\right] , \end{aligned} \tag{6.2}$$

where $\bar{\mathcal{A}}$ is the complex conjugate of $\mathcal{A}$, $f(r)$ and $g(r)$ are two real functions and f_1, f_2, g_1 and g_2 are radial perturbations around the background solutions. The deduction of the field equations is presented on Appendix C.

Imposing regularity at $r = 0$ we get the following boundary conditions at the origin

$$\begin{aligned} H_0(r) &= h_0 + \mathcal{O}(r^2)\,, \\ H_2(r) &= \mathcal{O}(r^2)\,, \\ f_1(r) &= h_1 r + \mathcal{O}(r^3)\,, \\ f_2(r) &= h_2 r + \mathcal{O}(r^3)\,, \\ g_2(r) &= \mathcal{O}(r^2)\,, \end{aligned} \tag{6.3}$$

where the coeficients h_0, h_1 and h_2 are constants. Using the linearity of the system (C.2)-(C.6), we can set $h_1 = 1$. We see from (C.5) that, when $\Omega = 0$, the function f_2 decouples from the others and h_2 is an arbitrary constant, so we can set it to zero and check a posteriori that this is consistent with the boundary conditions.

At infinity, the imposed boundary conditions are that all perturbed quantities approach zero for sufficiently large r, except for H_0 which approaches a constant positive value. In general, imposing two of these conditions was proved sufficient to ensure all the others.

Starting from one solution, found through the hypothesis that the point of maximum mass corresponds to $\Omega = 0$, we developed a code shooting for the parameters Ω and h_0, such that the solutions satisfy the boundary conditions. First it increments the value of f_0 and solves the system (3.22)-(3.25) ((4.13)-(4.16) for AdS), then it takes the solution and inserts it into (C.2)-(C.6) of which only the two refered parameters remain unknown.

Despite the similarities between the numerical method described here and the one used to find unperturbed solutions on chapters 3 and 4, the fact that the shooting method is now implemented for two parameters instead of one makes the code significantly more complicated and solutions are much harder to find. Furthermore, as the numerical code requires an initial guess for the values of the parameters to find the closest solution, we found that guesses need to be a lot more precise in this case for the computer to be able to find a solution at all.

6.2 Numerical results in asymptotically flat spacetime

Setting $\Lambda = 0$, the profile of Ω^2 as a function of the mass of the Proca star obtained numerically is shown on Figure 6.1. The black dot on Figure 6.1 denotes the point of maximum mass $1.087\ M_{Pl}^2/\mu^2$ shown also on Figure 3.4. It is visible that Ω is a real number for f_0 smaller than that which corresponds to the maximum ADM mass. These are the stable normal modes of the star. For f_0 larger than that, Ω becomes a pure positive imaginary number and thus, from (6.1) and (6.2), we conclude that these solutions are unstable.

Solutions that fit in the unstable branch are likely to migrate back to the stable one through a mechanism of "gravitational cooling" [46, 47, 48, 49, 39], which consists in radiating energy until f_0 decreases just enough to find a stable solution. Another plausible outcome is that the unstable configuration radiates completely until there is no self-gravitating structure anymore.

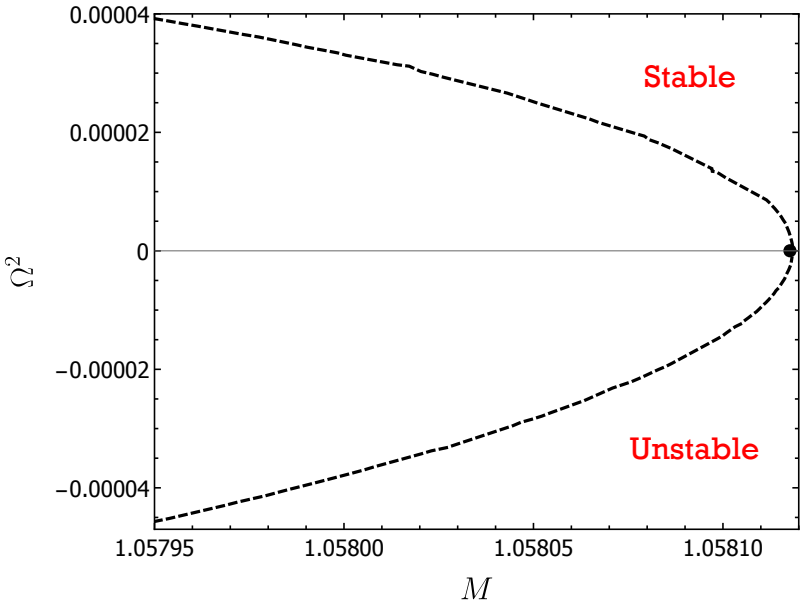

Figure 6.1: The squared characteristic vibrational frequency of the perturbation as a function of the total mass of the Proca star. The critical mass at which the star becomes unstable is also its point of maximum mass (black dot).

6.3 Numerical results is AdS

We performed the same study of stability for a Proca star in an asymptotically AdS spacetime with a cosmological constant of $\Lambda = -0.05\mu^2$. Although we expected roughly the same results as in the asymptotically flat case, the linear stability conditions of Proca stars in AdS are not yet described in the literature.

Proceeding much in the same way as was done before, we obtained a profile of the squared characteristic vibrational frequency of the star as a function of its mass (Figure 6.2). As expected, the same linear stability conditions apply to Proca stars in flat spacetime and in AdS, namely the star is stable for f_0 smaller than that which corresponds to the maximum mass and then becomes linearly unstable as the characteristic vibrational frequency becomes a pure positive imaginary number. One appreciable difference between the two cases is that, in AdS, the characteristic vibrational frequency changes significantly faster than in flat spacetime.

Unlike in the asymptotically flat case, where unstable solutions can become stable through mass ejection, the confining nature of the AdS spacetime makes this scenario impossible to occur for asymptotically AdS solutions. Hence, the most likely outcome would be the collapse to a black hole.

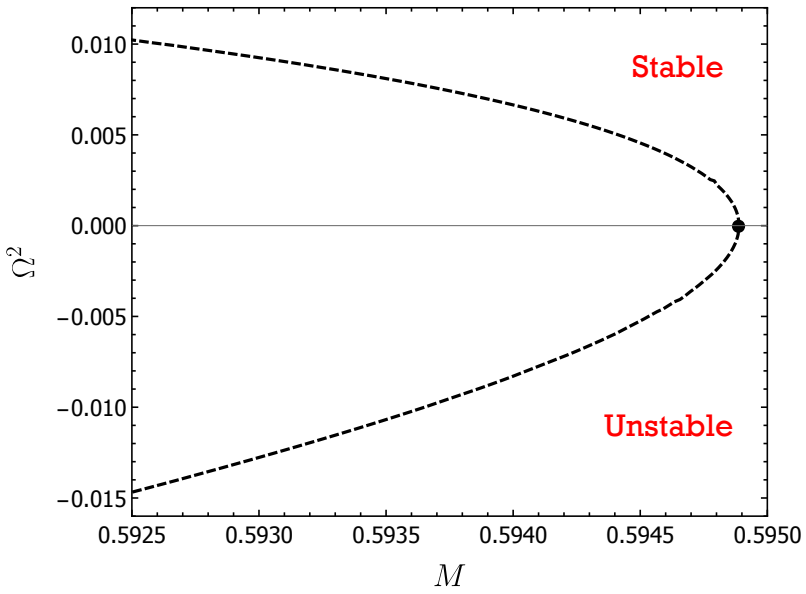

Figure 6.2: The squared characteristic vibrational frequency of the perturbation as a function of the total mass of the Proca star for $\Lambda = -0.05\mu^2$. The critical mass at which the star becomes unstable is also its point of maximum mass (black dot).

Chapter 7

Conclusions

7.1 Achievements

Throughout this thesis we found numerical solutions of self-gravitating spherically symmetric configurations of scalar and Proca bosons in both asymptotically flat and aAdS spacetimes. This way we showed that all these structures exhibit qualitatively similar results, as well as some noticeable differences. Namely, for both kinds of particles, the introduction of a negative cosmological constant decreases the maximum mass and particle number of the star. Moreover, the maximum mass reacheable by a star is larger for spin-1 particles than for scalar ones. Five-dimensional Proca star solutions were found and an instability of these objects in asymptotically flat spacetimes was argued based on the fact that the binding energy is positive for every solution.

With the goal of validating the numerical method, solutions of the Einstein-Klein-Gordon and the Einstein-Proca systems of equations were found analytically by considering the matter fields as perturbations of the background vacuum metric. Taking only terms of first order in the field, it was possible to obtain values of the frequency for the small amplitude regime which were in exceptional accordance with the numerical ones. To further ascertain this result, the ADM mass curve, as well as the one for the total particle number, calculated analytically were compared to the numerical points, which yielded, once again, satisfactory resemblance. Extrapolating the validity of the numerical method to regions far from the considered limit, this result grants confidence in the values thus obtained.

An extensive study of the stability of Proca stars in flat and AdS backgrounds was performed for linear spherically symmetric perturbations in the metric and the field components, with the result that, for values of f_0 lower than that which corresponds to the maximum mass, the star shows stability, while for larger ones it becomes linearly unstable.

Finally, a no-hair theorem was proved for spherically symmetric Proca stars in AdS stating that any collapse to a black hole in these conditions culminates necessarily in the Schwarzschild-AdS metric, that is, all the components of the energy-momentum tensor vanish.

The work presented here extends our knowledge on boson stars to the behaviour of Proca stars in aAdS spacetimes by showing that it is possible to have stable solitonic structures of spin-1 particles

in this spacetime, as well as asserting some of their fundamental properties. In the near future, this conclusion may not only prove useful in the context of the AdS/CFT correspondence, but also in further complementing our understanding of the stability of AdS spacetimes.

7.2 Future work

There are many possible extensions to the work done in this thesis. It should be possible to construct self-gravitating structures of real spin-1 fields in AdS, analogous to the scalar oscillons found in Refs. [23, 25]. In addition, it would be interesting to find out whether non-spherically symmetric rotating Proca stars can exist in AdS, much in the same way as was done for asymptotically flat spacetime in Ref. [15].

As stated on Section 4.2, massless spherically symmetric configurations of spin-1 fields in AdS do not exist. Although, it has recently been shown that one can construct static or stationary regular solutions of the Einstein-Maxwell system by dropping spherical symmetry [50, 51, 52]. It would then be an interesting development of this work to assert whether a massive version of these objects can exist in this spacetime.

Although most dynamical studies were mainly concerned with scalar fields [21, 22, 23, 24, 25], it is very likely that vector fields will show similar properties, several of which were indeed shown to be the same throughout this work. In particular, similarly to scalar boson stars, we expect Proca stars to be immune to the weakly turbulent instability.

The no-hair theorem shown on Appendix B states that spherically symmetric gravitational collapse results necessarily in the Schwarzschild-AdS metric. Nevertheless, we expect that it is possible to find solutions of Kerr-AdS black holes with Proca hair, in the same way as was done in Ref. [40] for asymptotically flat spacetime. This is only possible due to the fact that spherical symmetry is a prime assumption of the no-hair theorem. Also, one might expect to find massive generalizations of Einstein-Maxwell hairy black hole solutions in AdS [51, 53].

Concerning higher-dimensional gravity, further work could consist in rigorously establishing linear stability conditions for Proca stars in 4+1 dimensions. This could be done both for asymptotically flat spacetimes, in order to confirm the instability of all solutions argued on Section 4.3, and for asymptotically AdS spacetimes, with the likely result that the introduction of a negative cosmological constant creates a region of stable normal modes.

Finally, Ref. [54] argues that spherically symmetric scalar fields are not a good toy model for the general gravitational collapse of AdS spacetime, as opposed to gravitational perturbations. In that case, analogue spin-1 structures might provide a better model which is still simple enough to study.

Bibliography

[1] M. Duarte and R. Brito, 1609.01735.

[2] J. A. Wheeler, Phys. Rev. **97**, 511 (1955).

[3] D. J. Kaup, Phys. Rev. **172**, 1331 (1968).

[4] R. H. S. Budhi, S. Kashiwase and D. Suematsu, JCAP **1509**, 039 (2015), [1505.05955].

[5] S. Tsujikawa, Introductory review of cosmic inflation, in *2nd Tah Poe School on Cosmology: Modern Cosmology Phitsanulok, Thailand, April 17-25, 2003*, 2003, [hep-ph/0304257].

[6] R. Sharma, S. Karmakar and S. Mukherjee, Submitted to: Gen. Rel. Grav. (2008), [0812.3470].

[7] J. Lee, J. Korean Phys. Soc. **54**, 2622 (2009), [0801.1442].

[8] D. F. Torres, S. Capozziello and G. Lambiase, gr-qc/0012031.

[9] E. Berti and V. Cardoso, Int. J. Mod. Phys. **D15**, 2209 (2006), [gr-qc/0605101].

[10] C. F. Macedo, P. Pani, V. Cardoso and L. C. B. Crispino, Phys.Rev. **D88**, 064046 (2013), [1307.4812].

[11] M. Kesden, J. Gair and M. Kamionkowski, Phys. Rev. **D71**, 044015 (2005), [astro-ph/0411478].

[12] M. Pospelov and A. Ritz, Phys. Lett. **B671**, 391 (2009), [0810.1502].

[13] B. Holdom, Phys. Lett. **B166**, 196 (1986).

[14] N. Arkani-Hamed, D. P. Finkbeiner, T. R. Slatyer and N. Weiner, Phys. Rev. **D79**, 015014 (2009), [0810.0713].

[15] R. Brito, V. Cardoso, C. A. R. Herdeiro and E. Radu, Phys. Lett. **B752**, 291 (2016), [1508.05395].

[16] A. Proca, J. Phys. Radium **7**, 347 (1936).

[17] J. M. Maldacena, Int. J. Theor. Phys. **38**, 1113 (1999), [hep-th/9711200], [Adv. Theor. Math. Phys.2,231(1998)].

[18] P. Bizoń and A. Rostworowski, Phys. Rev. Lett. **107**, 031102 (2011), [1104.3702].

[19] J. Jalmuzna, A. Rostworowski and P. Bizoń, Phys. Rev. **D84**, 085021 (2011), [1108.4539].

[20] A. Buchel, L. Lehner and S. L. Liebling, Phys. Rev. **D86**, 123011 (2012), [1210.0890].

[21] O. J. C. Dias, G. T. Horowitz and J. E. Santos, Class. Quant. Grav. **29**, 194002 (2012), [1109.1825].

[22] O. J. C. Dias, G. T. Horowitz, D. Marolf and J. E. Santos, Class. Quant. Grav. **29**, 235019 (2012), [1208.5772].

[23] M. Maliborski and A. Rostworowski, Phys. Rev. Lett. **111**, 051102 (2013), [1303.3186].

[24] A. Buchel, S. L. Liebling and L. Lehner, Phys. Rev. **D87**, 123006 (2013), [1304.4166].

[25] G. Fodor, P. Forgács and P. Grandclément, Phys. Rev. **D92**, 025036 (2015), [1503.07746].

[26] G. H. Derrick, J. Math. Phys. **5**, 1252 (1964).

[27] R. Ruffini and S. Bonazzola, Phys. Rev. **187**, 1767 (1969).

[28] M. Colpi, S. L. Shapiro and I. Wasserman, Phys. Rev. Lett. **57**, 2485 (1986).

[29] E. W. Mielke and R. Scherzer, Phys. Rev. **D24**, 2111 (1981).

[30] P. Jetzer and J. J. van der Bij, Phys. Lett. **B227**, 341 (1989).

[31] A. Henriques, A. R. Liddle and R. Moorhouse, Phys.Lett. **B233**, 99 (1989).

[32] M. Gleiser, Phys.Rev.D **38**, 2376 (1988).

[33] T. Lee and Y. Pang, Nucl.Phys. **B315**, 477 (1989).

[34] S. Yoshida, Y. Eriguchi and T. Futamase, Phys.Rev. **D50**, 6235 (1994).

[35] S. L. Liebling and C. Palenzuela, Living Rev. Rel. **15**, 6 (2012), [1202.5809].

[36] L. D. Landau, Physik. Zeits. Sowjetunion 1 , 285 (1932).

[37] E. Seidel and W. Suen, Phys.Rev.Lett. **66**, 1659 (1991).

[38] D. N. Page, Phys.Rev. **D70**, 023002 (2004), [gr-qc/0310006].

[39] R. Brito, V. Cardoso, C. F. B. Macedo, H. Okawa and C. Palenzuela, Phys. Rev. **D93**, 044045 (2016), [1512.00466].

[40] C. Herdeiro, E. Radu and H. Runarsson, 1603.02687.

[41] K. Sakamoto and K. Shiraishi, Phys.Rev. **D58**, 124017 (1998), [gr-qc/9806040].

[42] D. Astefanesei and E. Radu, Nucl. Phys. **B665**, 594 (2003), [gr-qc/0309131].

[43] J. Balakrishna, E. Seidel and W.-M. Suen, Phys. Rev. **D58**, 104004 (1998), [gr-qc/9712064].

[44] B. Hartmann, B. Kleihaus, J. Kunz and M. List, Phys. Rev. **D82**, 084022 (2010), [1008.3137].

[45] Y. Brihaye and B. Hartmann, Class. Quant. Grav. **33**, 065002 (2016), [1509.04534].

[46] E. Seidel and W.-M. Suen, Phys.Rev. **D42**, 384 (1990).

[47] E. Seidel and W.-M. Suen, Phys.Rev.Lett. **72**, 2516 (1994), [gr-qc/9309015].

[48] M. Alcubierre *et al.*, Class.Quant.Grav. **20**, 2883 (2003), [gr-qc/0301105].

[49] R. Brito, V. Cardoso and H. Okawa, Phys. Rev. Lett. **115**, 111301 (2015), [1508.04773].

[50] C. Herdeiro and E. Radu, Phys. Lett. **B749**, 393 (2015), [1507.04370].

[51] M. S. Costa, L. Greenspan, M. Oliveira, J. Penedones and J. E. Santos, 1511.08505.

[52] C. Herdeiro and E. Radu, Phys. Lett. **B757**, 268 (2016), [1602.06990].

[53] C. A. R. Herdeiro and E. Radu, 1606.02302.

[54] O. J. C. Dias and J. E. Santos, 1602.03890.

[55] I. Peña and D. Sudarsky, Class. Quant. Grav. **14**, 3131 (1997).

Appendix A

Derrick's theorem

Derrick's theorem [26] uses a clever scaling argument to show that no regular static non-topological localized scalar field solutions are stable in flat spacetimes. In the following paragraphs, the theorem is rigorously stated and proved.

Definition 1. *A solution of the static Euler-Lagrange equations whose energy is finite and either the energy density is or the fields are asymtotically constant outside some finite region P is called a localised solution.*

Definition 1. *Any solution $\Phi(x)$ of the static Euler-Lagrange equations of a field theory for which*

$$\begin{aligned} \frac{d}{d\lambda} E_\lambda \Big|_{\lambda=1} &= 0\,, \\ \frac{d^2}{d\lambda^2} E_\lambda \Big|_{\lambda=1} &> 0\,, \end{aligned} \tag{A.1}$$

will be called a stable solution.

Theorem 1. *Let ϕ_a be the scalar fields and L the Lagrangian density of the model in question. Let the energy density of the model $E = E_2 + E_4 + E_0$ where*

$$\begin{aligned} E_0 &= g(\Phi)\,, \\ E_2 &= ||\partial_j \Phi||^2\,, \\ E_4 &= f(\Phi)\partial_j\phi^a\partial_k\phi^b\partial_l\phi^c\partial_m\phi^d M^{jklm}_{abcd}(\Phi)\,. \end{aligned} \tag{A.2}$$

Here g and M are such smooth maps $P \to C$ that the corresponding integrals E_2, E_4 and E_0 are finite and positive. Then the full Lagrangian density does not have stable, static, localised solutions if

$$(2-D)E_2 + (4-D)E_4 - DE_0 \neq 0\,, \tag{A.3}$$

or

$$(2-D)(1-D)E_2 + (4-D)(3-D)E_4 + D(D+1)E_0 \leq 0\,. \tag{A.4}$$

Proof. Let $\lambda > 0$ and let us assume that Φ is a static, localised solution of the Euler-Langrange equations of L. $E = E(\Phi) = \int d^D x(E_2 + E_4 + E_0) < \infty$ due to locality of Φ.

Let us perform a uniform scaling of the solution Φ so that $\Phi \to \Phi_\lambda$ and

$$E \to E_\lambda = \int d^D c \left(||\partial_j \Phi_\lambda||^2 + \partial_j \phi^a_\lambda \partial_k \phi^b_\lambda \partial_l \phi^c_\lambda \partial_m \phi^d_\lambda M^{jklm}_{abcd}(\Phi_\lambda) + g(\Phi_\lambda) \right) . \tag{A.5}$$

After a change of integration variables from x to $y = \lambda x$ we obtain

$$E_\lambda = \lambda^{2-D} E_2 + \lambda^{4-D} E_4 + \lambda^{0-D} E_0 \,, \tag{A.6}$$

This is a (possibly local) minimum under variation of λ if and only if

$$\left(\frac{d}{d\lambda} E_\lambda \right) = (2-D)E_2 + (4-D)E_4 - DE_0 = 0 \,, \tag{A.7}$$

and

$$\left(\frac{d^2}{d\lambda^2} E_\lambda \right) = (2-D)(1-D)E_2 + (4-D)(3-D)E_4 - D(D+1)E_0 > 0 \,. \tag{A.8}$$

Since Φ is a solution, this completes the proof.

Appendix B

A no-hair theorem for Proca stars in AdS

Peña and Sudarsky [55] proved that a black hole resulting from spherically symmetric regular scalar boson star configurations in an asymptotically flat spacetime is necessarily trivial. Hence, any configuration that collapses gravitationally, culminates in the Schwarzschild spacetime (T^{ν}_{μ}=0). Following similar arguments, Ref. [42] presents a generalization of the theorem for a negative cosmological constant. Although, the proof of such a theorem is a little more cumbersome when the scalar field is replaced by a spin-1 field. Here we prove a no-hair theorem for Proca stars in aAdS spacetimes, following the same arguments as those in Ref. [40].

Let us assume a regular black hole solution of Einstein's equations. Such geometry would have a regular horizon, say at $r = r_H$, such that $F(r_H) = 0$, since $r = r_H$ describes a null hypersurface. Assuming there are no more exterior horizons, $F'(r_H) > 0$. Also, we can assume $\sigma(r)$ to be strictly positive since the equations of motion (4.13)-(4.16) are invariant under a sign change of that function. Therefore, $F(r)$ and $\sigma(r)$ are two always positive functions. Taking the expression for the energy density of the fields,

$$-T^t_t = \frac{(f' - \omega g)^2}{2\sigma^2} + \frac{1}{2}\mu^2\left(g^2 F + \frac{f^2}{F\sigma^2}\right) , \tag{B.1}$$

we see that $f(r_H) = 0$, by imposing regularity at the horizon. Hence we can assume that f is a strictly increasing and positive function in some interval $r_H < r < r_1$ (or decreasing and negative, which leads to the same results).

Let us now write (4.14) as

$$f' = \omega g\left(1 - \frac{\mu^2\sigma^2 F}{\omega^2}\right) . \tag{B.2}$$

Note that for $r = r_H$, the part multiplied by ωg is 1, so it is clear that in some interval $r_H < r < r_2$, that part is strictly positive. Writing the Lorentz condition explicitly we obtain

$$r^2\sigma F g = -\omega\int_{r_H}^{r} dx \frac{x^2 f}{\sigma F} , \tag{B.3}$$

which is negative in $r_H < r < r_c$, where r_c is the minimum between r_1 and r_2. Hence, $g < 0$, which is impossible given (B.2). We thus conclude that $f(r) = g(r) = 0$ and the only black hole solution allowed by these equations of motion is the Schwarzschild-AdS spacetime.

Appendix C

Linear stability analysis: field equations

Expanding the field equations at first order in the perturbed quantities, we find that the (tr) component of the Einstein equations gives

$$g_1 = -\frac{2g\mu^2 f_2 + i\Omega H_2}{2\mu^2 f} \,. \tag{C.1}$$

Replacing this in the (tt) component we get:

$$\begin{aligned} H_2' =& H_2\left(\frac{r\mu^2 f^2}{F^2\sigma^2} - \frac{1}{rF} - \frac{\Omega^2 g}{\omega f} + \frac{\Lambda r}{F}\right) + H_0\left(\frac{r\mu^2 f}{F^2\sigma^2} + \frac{r\mu^4 g^2 F\sigma^2}{\omega^2}\right) + 4g\mu^2 g_2 + f_2\frac{2i\mu^2\Omega g^2}{\omega f} + \\ & 2\mu^2 f_1\left(\frac{g}{r\omega} + \frac{f}{\sigma^2 F^2}\right) - f_1'\frac{2\mu^2 g}{\omega} \,, \end{aligned} \tag{C.2}$$

Multiplying the (rr) component by $F^2\sigma^2$ and adding the (tt) component one finds

$$H_0' = H_2' - 4g\mu^2 g_2 - (H_0 + H_2)\frac{2r\mu^2 f^2}{F^2\sigma^2} - f_1\frac{4\mu^2 f}{F^2\sigma^2} \,. \tag{C.3}$$

The (r) component of the Proca field equations and its complex conjugate are independent and give

$$\begin{aligned} f_1' =& \frac{f_1}{r} + g_2\omega\left(1 - \frac{\mu^2 F\sigma^2}{\omega^2 - \Omega^2}\right) + H_0\frac{\mu^2 rgF\sigma^2(2\omega^2 - \Omega^2)}{2\omega(\omega^2 - \Omega^2)} + f_2\frac{i\Omega g(\mu^2 F\sigma^2 + \omega^2 - \Omega^2)}{f(\omega^2 - \Omega^2)} + \\ & \frac{H_2\Omega^2}{2f}\left[\frac{F\sigma^2(\mu^2 rfg - \omega)}{\omega^3 - \omega\Omega^2} - \frac{1}{\mu^2}\right] \,, \end{aligned} \tag{C.4}$$

$$\begin{aligned} f_2' =& -i\Omega g_2\omega\left(1 + \frac{\mu^2 N\sigma^2}{\omega^2 - \Omega^2}\right) + H_0\frac{i\Omega\mu^2 rgF\sigma^2}{2(\omega^2 - \Omega^2)} + f_2\left[\frac{1}{r} + \frac{\omega g(\omega^2 - \Omega^2 - \mu^2 F\sigma^2)}{f(\omega^2 - \Omega^2)}\right] + \\ & \frac{iH_2\Omega}{2f}\left[\frac{F\sigma^2(\mu^2 rfg - \omega)}{\omega^2 - \Omega^2} + \frac{\omega}{\mu^2}\right] \,. \end{aligned} \tag{C.5}$$

Substituting in order to erase all derivatives from the right hand side of the expression we finally get, from the (t) component of the Proca equations

$$\begin{aligned} g_2' = &- f_1 \frac{\omega}{F^2\sigma^2} + g_2 \left[\frac{\mu^4 r g^2 F \sigma^2 (3\omega^2 - \Omega^2)}{\omega^2(\omega^2 - \Omega^2)} - \frac{1}{rF} + \frac{r\Lambda}{F} \right] + H_0 \left(- \frac{r\omega f}{F^2\sigma^2} - \frac{\mu^4 r^2 g^3 F \sigma^2}{\omega^2 - \Omega^2} \right) + \\ & H_2 \left[\frac{\mu^2 r \Omega^2 g^2 F \sigma^2 (\omega - \mu^2 r f g)}{\omega^2 f (\omega^2 - \Omega^2)} - \frac{r\omega f}{F^2\sigma^2} - \frac{g}{F} + \frac{r^2 \Lambda g}{F} \right] + \frac{i\Omega f_2}{F^2\sigma^2} \left(\frac{2\mu^4 r g^3 F^3 \sigma^4}{\omega^3 f - \omega \Omega^2 f} + 1 \right) . \end{aligned} \tag{C.6}$$

We see that, although there are six perturbed functions, (C.1) already gives us g_1 as a function of the others so we can consider (C.2)-(C.6) as the full set of equations.